Title

A Surface Science and Catalytic Study of the Effects of Aluminum Oxide and Potassium on the Ammonia Synthesis over Iron Single-Crystal Surfaces

Journal

Catalytic Ammonia Synthesis: Fundamentals and Practice, Chapter 4

Authors

Strongin, D.R.
Somorjai, Gabor A.

Publication Date

1991

Lawrence Berkeley Laboratory
UNIVERSITY OF CALIFORNIA

Materials & Chemical Sciences Division

To be published as a chapter in
Catalytic Ammonia Synthesis: Fundamentals and Practice, J.R. Jennings, Ed.,
Plenum Publishing Company, London, England

A Surface Science and Catalytic Study of the Effects of Aluminum Oxide and Potassium on the Ammonia Synthesis over Iron Single Crystal Surfaces

D.R. Strongin and G.A. Somorjai

July 1987

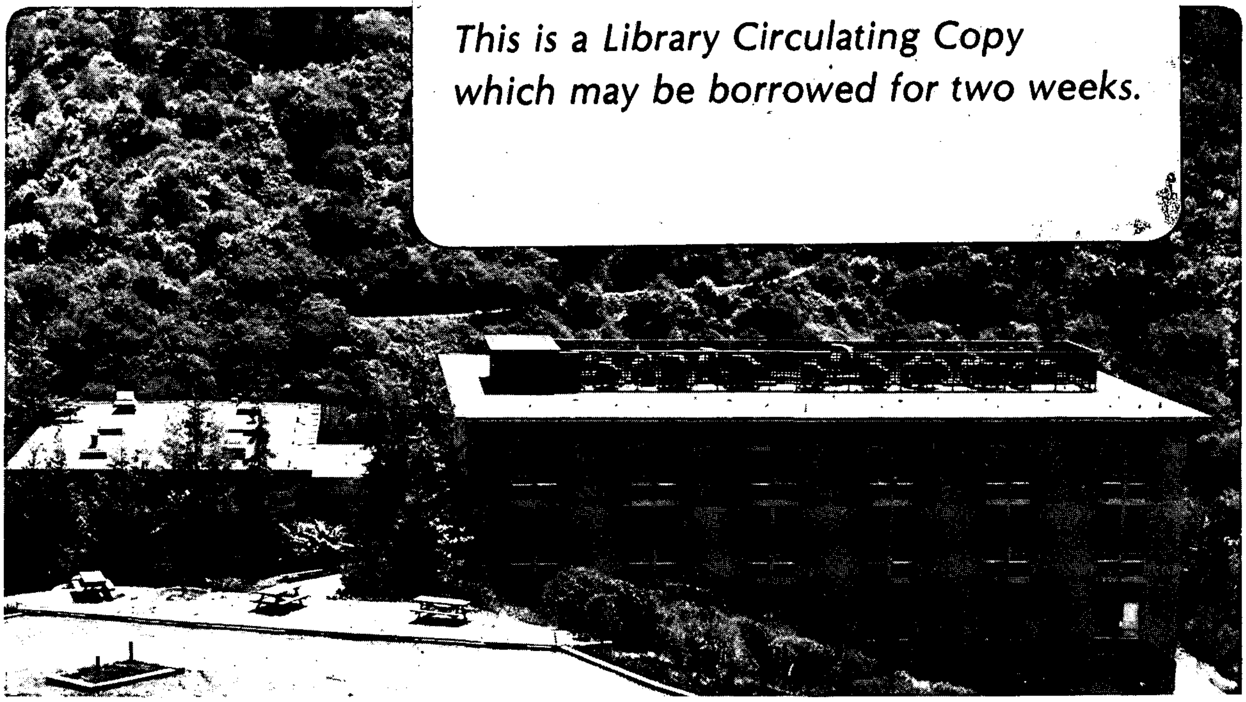

Prepared for the U.S. Department of Energy under Contract DE-AC03-76SF00098

A Surface Science and Catalytic Study of the Effects of Aluminum Oxide and Potassium on the Ammonia Synthesis Over Iron Single Crystal Surfaces

D. R. Strongin and G. A. Somorjai

Department of Chemistry
University of California
Berkeley, California 94720
and
Materials and Chemical Sciences Division
Lawrence Berkeley Laboratory
Berkeley, California 94720

Contents

1 Introduction

Present-day ammonia synthesis is the product of close to a century worth of research. Much of the effort has been directed toward elucidating the promoter effects of potassium and aluminum oxide on the rate of ammonia synthesis. Out of this work has evolved a multitude of techniques, concepts, and ideas which have profoundly affected catalytic chemistry. Many reviews have been written on this subject[1,2,3], but it becomes evident from them that a molecular level understanding of the promoters is still lacking. A principal reason for this deficiency is that the bulk of this early work has used indirect methods to study the catalyst. A large amount of kinetic data relating the gas phase ammonia concentration to the surface concentration of promoters has been obtained [4,5]. This type of data is important for optimizing the concentration of promoters but it fails to reveal the atomic level effects of the promoters on the working catalyst. With the advent of combined surface science /high pressure systems, high pressure reaction data($>$1 atmosphere) can be correlated to the atomic structure of the catalyst surface which is determined in the ultra-high vacuum environment($< 10^{-8}$ Torr). The combination of surface science and high pressure catalysis provides powerful tools in the study of the reactivity and structure of surfaces. This chapter will be devoted to describing how surface science work, combined with high pressure data, has elucidated the structure sensitivity and the role of potassium and aluminum oxide in ammonia synthesis. The structure sensitivity of ammonia synthesis will be presented first since it serves as necessary background when explaining potassium and aluminum oxide promotion in ammonia synthesis.

2 Composition of the Industrial Catalyst

Since the realization of industrial scale ammonia synthesis in 1916 there have been no major changes in the composition of the iron synthesis catalyst[2,6]. Potassium oxide and aluminum oxide are fused with magnetite followed by reduction.

The reduction procedure involves treating the oxidized catalyst with a stoichiometric mixture of nitrogen and hydrogen[1,7]. The temperature and extent to which this is carried out is dependent on the concentration of potassium and aluminum oxide in the iron oxide. About 1-3% of K_2O and Al_2O_3 are usually used and following reduction anywhere between 40-60% of the iron is covered by the promoters[8,9,10,7]. Previous work has determined that Al_2O_3 increases the surface area of the catalyst from a value of 1 m^2/g-cat. for unpromoted iron to 20m^2/g-cat.[2] when aluminum oxide is added (so called structural promotion). Potassium decreases the surface area to about 10 m^2/g-cat. but the activity of the catalyst increases by a factor of three (so called electronic promotion)[2].

3 Experimental

3.1 The Need for a Model System

It is apparent that the ammonia synthesis catalyst is a complex mixture of iron, potassium, aluminum, and oxygen, and that the promotion by Al_2O_3 and K_2O comes through an interaction with the active iron component[7]. If a complex system such as this is to be understood it is advisable to study a model system. In this case iron single crystals prepared and characterized in UHV were used to model the active component of the industrial catalyst. By quantitatively adding potassium, aluminum and oxygen to the single crystal surface in UHV and then carrying out high pressure ammonia synthesis (20 atm of nitrogen and hydrogen), direct correlation can be made between reactivity and surface structure of the catalyst.

3.2 Preparation and Characterization of Well Defined Single Crystal Surfaces in Ultra - High Vacuum

The single crystal samples used in our work are on the average $1cm^2$ disks about 1mm thick. They are polished on both sides by standard metallurgical techniques to provide a surface smooth on the micron scale. The crystal can be heated resistively and the temperature of the sample is measured by a chromel-alumel thermocouple which is spot-welded to the crystal edge. In the case of iron, bulk impurities such as sulfur and carbon are common. Before the sample is mounted in UHV the crystal is heated to about 873K in a hydrogen furnace to help deplete the bulk of sulfur. The cleaning procedure is continued in UHV where a combination of argon ion sputtering and chemical treatment is used.

Sputtering the iron at 873K for a prolonged period of time removes the sulfur but treatment of the sample in about 1×10^{-7} Torr of oxygen at 673K is needed to rid the sample of carbon. The iron surface is considered clean if Auger electron spectroscopy(AES) shows no impurities and if a low energy electron diffraction pattern (LEED) is obtained which is representative of the bulk crystal orientation.

Aluminum is evaporated on the iron crystal surface by heating a ceramic crucible containing aluminum wire. The aluminum is oxidized on the iron surface by leaking about 1×10^{-8} Torr of water vapor into the UHV chamber. Oxidation of the aluminum is confirmed by the shift of the 67eV LVV Auger transition, representative of elemental aluminum, to 54eV in the oxide[11]. The coverage of aluminum oxide is determined by titrating the surface with carbon monoxide. At room temperature CO chemisorbs on metallic iron but not on aluminum oxide[2,12]. By adsorbing and desorbing CO from both clean iron and Al_xO_y/Fe surfaces, the relative amount of free iron can be calculated(aluminum oxide is denoted by Al_xO_y because of uncertainty in the aluminum and oxygen stoichiometry). The Auger spectrum can be calibrated using this data so that coverages of aluminum oxide can be alternatively determined by AES. In this work, one monolayer corresponds to the point at which

CO can no longer adsorb to the surface. Thus, one monolayer might correspond to more than one atomic layer since aluminum oxide grows in three-dimensional islands on the iron surface[13]. The deposition of potassium is accomplished by using a Saes getter source. Coverages of potassium are determined by a potassium uptake curve.

3.3 Combined UHV/High Pressure Apparatus

After the sample is prepared and characterized in UHV it must be transferred to a different environment if ammonia synthesis is to be studied since the rate of ammonia production from its elements would be negligible in UHV. Having a UHV chamber equipped with a high pressure cell[14] provides the necessary environment while never exposing the sample to the ambient atmosphere. A typical experiment would proceed as follows. The sample is cleaned and potassium and aluminum oxide are added in the desired concentrations on the iron surface. The single crystal is enclosed in a high pressure cell which constitutes part of a micro-batch reactor, isolating the sample from the UHV environment. High pressures of gases (15 atm of hydrogen and 5atm of nitrogen) are introduced and the sample is resistively heated to reaction temperature (673K unless otherwise noted). Ammonia production is monitored by periodically taking samples from the reaction loop and passing them through a photoionization detector with a 10.2 eV lamp. This photon energy ionizes ammonia but not nitrogen and hydrogen. Thus the PID signal is only proportional to the ammonia partial pressure in the loop. By taking these samples at known times rates of ammonia synthesis are determined. After the reaction is completed, the reaction loop is evacuated and the cell opened returning the sample to the UHV environment where surface characterization is performed by AES, LEED, and temperature programmed desorption (TPD).

4 Structure Sensitivity of the Ammonia Synthesis

Since single crystals have a surface with a well defined geometry the structure sensitivity of a reaction can be probed directly. This approach has proved effective in many systems[15] where it has been found that surface geometries influence catalytic reactions. This is best exemplified in ammonia synthesis where differences of up to two orders of magnitude are found between crystallographic planes[16]. The rates of ammonia synthesis are shown over five iron crystal orientations in figure 1. The Fe(111) and Fe(211) surfaces are by far the most active in ammonia synthesis, and they are followed in reactivity by Fe(100), Fe(210), and Fe(110)[17]. Schematic representations of the idealized unit cells for these surfaces, shown in figure 2, suggest two possible reasons for the high activity of the (111) and (211) faces compared to the (210), (100) and (110) orientations; surface roughness or active sites.

The (111) surface can be considered a rough surface since it exposes second and third layer atoms to reactant gases in contrast to the (110) surface which only exposes first layer atoms. Work functions are related to the roughness of a surface[18] and it is usefull to quantify the corregation of a plane in this way. The work functions of all the iron faces are not available but they are for tungsten[19], another bcc metal which shows structure sensitivity for ammonia decomposition[20]. The order of decreasing work function(ϕ) is as follows; $\phi_{110} > \phi_{211} > \phi_{100} > \phi_{111} > \phi_{210}$. Open faces, like the (111) surface, have lower work functions than close packed faces such as the (110) surface. The significance of this for ammonia synthesis might be that the dissociation of dinitrogen (the rate limiting step[21,22]) proceeds faster on a surface with a low work function. This is supported by theory[21], which calls for transfer of electronic charge from the d band of iron into the $2\pi^*$ antibonding orbitals of dinitrogen for dissociation, a process which might be aided by a low work function.

The second possible explanation for the structure sensitivity involves active sites. The (111) and (211) faces of iron are the only surfaces which expose C_7 sites(iron atoms with seven nearest neighbors) to the reactant gases. Theoretical work by Falicov et. al.[23] has suggested that highly coordinated surface atoms would show increased catalytic activity due to low energy charge fluctuations in the d bands of highly coordinated surface atoms. Examination of the results suggest that the latter argument of active sites is the key to the structure sensitivity of ammonia synthesis over iron.

The reaction rates, in figure 1, show that the (211) face is almost as active as the (111) plane of iron, while Fe(210) is less active than Fe(100). The Fe(210) and Fe(111) faces are open faces which expose second and third layer atoms. The Fe(211) face is more close packed, but it exposes C_7 sites. If surface roughness or a low work function were the important consideration for an active ammonia synthesis catalyst, then the Fe(210) would of been expected to be the most active face. Instead Fe(111) and Fe(211) are much more active, indicating that the presence of C_7 sites are more important than surface roughness in an ammonia synthesis catalyst.

The idea of C_7 sites being the most active site in ammonia synthesis on iron has been suggested in the past. Dumesic *et al.*[24] found that the turnover number for ammonia synthesis was lower on small iron particles than larger ones. Pretreatment of an Fe/MgO catalyst with ammonia enhanced the turnover number over small iron particles, but did not affect the larger particles. This result was explained by noting that the concentration of C_7 sites would be expected to be higher on the smaller iron particles and that the ammonia induced restructuring enhanced the number of these sites on the catalyst. This was supported by the fact that the restructured catalyst chemisorbed 10% less CO than the unrestructured catalyst. Highly coordinated sites, such as C_7, would chemisorb less CO than less coordinated sites because of steric considerations. Thus, it was concluded that C_7 sites are the most active iron atoms for ammonia synthesis.

Additional research which supports the contention that highly coordinated surface sites are most active for ammonia synthesis has been carried out on rhenium[25].

In this study the rate of ammonia synthesis over the (0001), $(10\bar{1}0)$, $(11\bar{2}0)$, and $(11\bar{2}1)$ faces were determined (fig.3). Here, as in the case of iron the face with the highest activity, the $(11\bar{2}1)$ plane, is the surface which exposes the most highly coordinated sites. Figure 3 also shows that the $(11\bar{2}1)$ face exposes C_{11} and C_{10} sites while the next active $(11\bar{2}0)$ face exposes C_{11} and C_7 sites. This work, taken along with the work on the iron crystal faces, support the contension that highly coordinated sites are those which are most active for ammonia synthesis and that surface roughness is only important to the extent that it can expose these active surface atoms to the gas phase nitrogen and hydrogen.

5 Surface Science Studies of K/Fe, $K/N_2/Fe$, and $K/NH_3/Fe$ Systems

This section summarizes a large amount of work which has been performed outside our laboratory(except for section 5.4). The structure and bonding strength of potassium will be discussed along with the effect of potassium on the dissociative chemisorption of dinitrogen on iron single crystal surfaces.

5.1 The Structure of Potassium on Iron Single Crystal Surfaces

The structure of potassium overlayers on well-defined single crystal surfaces[26,27] has been investigated. Potassium shows no ordered structures on the (100) face of iron at any surface coverage. Ordered overlayers have been observed for potassium adsorbed on Fe(110) and Fe(111).

At a saturation coverage of potassium, a hexagonal close-packed ordered overlayer has been observed on the (110) face of iron. A lack of ordering by potassium is found at lower coverages and this is usually explained by noting that the mobility of the alkali metal on the iron surface is high. This allows only small ordered domains to exist which can not be observed by LEED. At higher coverages lateral interactions between neighboring adsorbed potassium atoms result, and hence the potassium resides in energetically favorable surface sites which form an ordered structure.

In contrast, the (111) surface of iron exhibits an ordered potassium structure only at low potassium coverages where a (3×3) structure is observed. At higher coverages of potassium, the diffraction pattern corresponding to the (3×3) structure deteriorates and a (1×1) structure results, with a high background that indicates the presence of disordered potassium.

5.2 The Stability of Potassium on Iron in UHV

The strength of the interaction between iron and potassium has been studied by temperature programmed desorption[26,27]. Potassium TPD spectra from the (111), (100), and (110) faces of iron show the same qualitative features. At low coverages of potassium($\theta_K \approx 0.07$, where θ_K is equal to the number of potassium atoms divided by the number of surface Fe atoms), desorption occurs $\gtrsim$800K, but with higher coverages($\theta_K \approx 0.8$) of potassium, the maximum rate of desorption decreases to about 550K(fig.4). This type of behavior is common for alkalis on transition metals. Reneutralization of the alkali metal begins to occur[28] as higher coverages of potassium are achieved, resulting in a lower iron - potassium interaction, and hence a reduction in the desorption energy. Using the Redhead analysis[29], the desorption energies of potassium on the various iron crystal faces are as follows: Fe(110), 57±2kcal/mole; Fe(100), 54±2kcal/mole; Fe(111), 52±2kcal/mole. These values are obtained by extrapolating to zero coverage so they are upper limits for the strength of the potassium - iron bond. Desorption energies will become lower at higher coverages of potassium, but detailed data necessary to determine the potassium desorption energy as a function of coverage is not available.

Coadsorption of oxygen thermally stabilizes the potassium on the iron surface as exhibited in figure 5. These TPD spectra show that for high coverages of potassium the coadsorption of oxygen appreciably raises the desorption temperature. For a potassium adlayer without oxygen, the maximum desorption rate occurs at 550K and all the potassium desorbs by 900K. When oxygen is present, the maximum rate of desorption is increased in temperature to 750K, and even at 1000K, part of the potassium-oxygen adlayer is thermally stable on the iron surface. It is also evident from the figure that the order of adsorption of potassium and oxygen does not significantly change the thermal stability of the adlayer at high coverages of both components. However, at lower coverages of potassium and oxygen, the order of adsorption of the additives does change the thermal stability of the layer. If oxygen is predosed($Y_0=0.48$, $Y_0=\frac{Auger intensity of O 510eV peak}{Auger intensity of Fe 650eV peak}$) on a polycrystalline iron followed by the addition of potassium($n_K=1.48\times10^{14}cm^{-2}$), then the maximum rate of potassium desorption occurs at 750K. On a surface where potassium is added first($n_K=1.55\times10^{14}cm^{-2}$), followed by oxygen addition($Y_0=0.89$), the maximum rate of potassium desorption occurs at about 800K. In addition a much larger fraction of the potassium desorbs above 1000K when potassium is present on the surface before the addition of oxygen.

The nature of the K + O adlayer is uncertain, but research[30] on Fe(110), using XPS and UPS has shown that oxygen is directly bound to the iron surface. The interaction between the potassium and the oxygen, probably responsible for the thermal stability of the layer, was observed as a shift in the potassium 2p level in the XPS studies. These results suggest that the potassium and oxygen exist as an adlayer in which the potassium and oxygen are both chemisorbed directly to the iron surface or in a configuration where the potassium sits on top of an oxygen layer. The fact that the adlayer is more stable when potassium is adsorbed on the iron before the addition of oxygen is strong evidence for the former case. The formation of a bulk potassium compound, such as K_2O, is extremely unlikely since this compound is known to decompose at about 620K. This decomposition temperature is well below 1000K, where the potassium - oxygen layer is stable in the TPD experiments.

5.3 The Effect of Potassium on the Dissociative Chemisorption of Nitrogen on Iron Single Crystal Surfaces in UHV

The rate determining step in the ammonia synthesis is accepted to be the dissociation of dinitrogen[21,3,5]. The interaction between nitrogen and iron has been studied[31,32] along with the addition of submonolayer amounts of potassium[33,21,34]. All the work that will be mentioned has been carried out in a UHV chamber, limiting the pressure range to be between 10^{-4} - 10^{-10} Torr.

Using iron single crystals and polycrystalline foils, the sticking probability of nitrogen on iron was found to be on the order of 10^{-7}. This result reveals why, in addition to thermodynamic considerations, ammonia synthesis from the elements is favored at high reactant gas pressures. Since the sticking probability of dissociating dinitrogen is so low on iron, higher pressures of nitrogen enhances the kinetics of the rate limiting step in ammonia synthesis. The structure sensitivity of the reaction(see section 4) is also revealed in the nitrogen chemisorption studies. It was found that the Fe(111) surface dissociatively chemisorbed nitrogen 20 times faster than the Fe(100) surface and 60 times faster than the Fe(110) surface. This agrees well with the structure sensitivity of ammonia synthesis and adds more credence to dissociative chemisorption being the rate limiting step. The addition of submonolayer amounts of elemental potassium has drastic effects on the nitrogen chemisorption properties of the (110), (100) and (111) faces of iron.

Figure 6[34] shows the effect of potassium on the initial sticking coefficient(σ_o) of dinitrogen on a Fe(100) surface. For clean Fe(100), $\sigma_o \approx 1.4\times10^{-7}$, but with the addition of potassium σ_o increases almost linearly, until a potassium concentration of 1.5×10^{14}K atoms/cm^2, where σ_o maximizes at a value of 3.9×10^{-5}; a factor of 280 enhancement. Higher coverages of potassium start to decrease σ_o, presumably due to potassium blocking iron sites which would otherwise dissociatively chemisorb dinitrogen. The maximum increase in σ_o, due to potassium adsorption, on Fe(111) is about a factor of 8(σ_o=4×10^{-5}) at a potassium concentration of 2×10^{14}K atoms/cm^2(fig. 7). The potassium induced enhancement of σ_o on the Fe(110) surface is greater than that observed on either Fe(111) or Fe(100), so that the differences in activities for dinitrogen dissociation seen on the clean surfaces is eliminated in the presence of potassium.

The mechanism by which potassium promotes dinitrogen chemisorption is usually attributed to the lowering of the surface work function in the vicinity of a potassium iron. This effect is greatest at coverages low enough($\lessapprox$ 0.15) where the potassium - iron bond has strong ionic character so that the local ionization potential of the surface iron atoms is greatest. This allows for more electron density to be transferred to the dinitrogen $2\pi^*$ antibonding orbitals from the surface. This phenomenon increases the adsorption energy of molecular nitrogen and simultaneously lowers the activation energy for dissociation. For example, on the Fe(100) surface the addition of 1.5×10^{14}K atoms/cm^2 decreases the work function by about 1.8eV and increases the rate of dinitrogen dissociation by more than a factor of 200. This enhancement in rate is accompianed by an increase in the adsorption energy of dinitrogen on Fe(100) by 11.5kcal/mole, which decreases the activation barrier for dissociation, in the presence of potassium, from 2.5kcal/mole to about 0kcal/mole.

The coadsorption of oxygen has been found to decrease the promoter effect of potassium on the rate of dinitrogen dissociation over iron. Figure 8 shows that σ_o decreases continuously with increasing oxygen coverage on a polycrystalline iron sample. The effect of the oxygen on nitrogen adsorption, in this study, is attributed to the physical blockage of iron surface, since if σ_o is normalized to the amount of iron surface which is accessible to dinitrogen, then σ_o remains fairly constant as oxygen coverages are increased. This result implies that the promoter effect of potassium is not significantly affected by the presence of oxygen. It is also strong evidence for an adlayer where both potassium and oxygen interact directly with the iron surface, since potassium sitting on top of oxygen would not be expected to exert the same promotion as potassium adsorbed alone.

5.4 Ammonia Temperature Programmed Desorption Studies on K/Fe

The temperature programmed desorption of ammonia from clean Fe(111) and K/Fe(111) is shown in figure 9[35]. Ammonia desorbs through a wide temperature range resulting in a broad peak with a maximum rate of desorption occurring at around 300 K. With the addition of 0.1ML of potassium, the peak maximum shifts about 40 K. Using the Redhead analysis[29] and assuming first order desorption for ammonia, the 40 K decrease corresponds to a 2.4kcal/mole drop in the adsorption energy of ammonia on iron in the presence of 0.1ML potassium. The peak maximum continuously shifts to lower temperature with increasing amounts of coadsorbed potassium. At a coverage of 0.25ML a new desorption peak grows in at about 189 K. Increasing coverages of potassium now increase the intensity of the new peak(it also shifts to lower temperatures) and decreases the intensity of the original ammonia desorption peak. At a potassium coverage of about 1.0ML only a weakly bound ammonia species is present with a maximum rate of desorption occurring at 164 K. This observation of ammonia adsorption energy decreasing with the coadsorption of potassium on iron is similar to what is found for ammonia desorption from nickel and ruthenium with adsorbed sodium[36,37].

5.5 Summary of Surface Science Results

Many conjectures on the chemical state and role of potassium in ammonia synthesis can be made from the surface science results. The potassium TPD results clearly show that elemental potassium will not be stable at the temperatures necessary to perform the synthesis of ammonia. The industrial reaction is usually run between 673K and 748K and the TPD results show that elemental potassium would rapidly desorb at these temperatures. With the coadsorption of oxygen, potassium can be thermally stabilized up to temperatures greater than 1000K. Bulk potassium compounds such as K_2O or KOH would not be stable under ammonia synthesis conditions[38]. This suggests that the addition of K_2O to the industrial catalyst results in a chemisorbed potassium and oxygen adlayer, stable under industrial ammonia synthesis conditions.

The (111) face of iron has been shown to dissociatively chemisorb dinitrogen 20 times faster than Fe(100) and 60 times faster than Fe(110). The addition of potassium increases the rate of dinitrogen dissociation over Fe(100) and Fe(110) by more than an order of magnitude. The effect over Fe(111) is much less pronounced, so that the differences in activities, observed over the clean surfaces, is eliminated in the presence of potassium.

Although vital for thermally stabilizing potassium, the presence of oxygen decreases the rate of dinitrogen dissociation on iron because it physically blocks iron surface. A rough inverse proportionality is observed between σ_o, the initial sticking coefficient of dinitrogen on K/Fe, and the coverage of oxygen. The K + O adlayer is expected to promote ammonia synthesis by enhancing the rate limiting step. The high pressure studies presented next suggest that a more important promoter effect of potassium involves lowering the concentration of adsorbed ammonia on the iron catalyst, thus making more sites available for the dissociation of dinitrogen. This is supported by the ammonia TPD results which show that potassium substantially decreases the adsorption energy of ammonia on iron. Even in the presence of only 0.1ML of potassium, the adsorption energy of ammonia is reduced by 2.4kcal/mole.

6 Combined Surface Science and Catalytic Study of the Effects of Potassium on the Ammonia Synthesis

6.1 Effects of Potassium on Ammonia Synthesis Kinetics

An extensive amount of work has been completed which determined the effects of potassium on ammonia synthesis over iron single crystal surfaces of (111), (100), and (110) orientations[35]. The apparent order of ammonia and hydrogen for ammonia synthesis over Fe and K/Fe surfaces have been determined in addition to the effect of potassium on the apparent activation energy(E_a) for the reaction. In all the experiments which will be mentioned, potassium was coadsorbed with oxygen[39,40]. Elemental potassium is not stable and only about 0.15ML of potassium coadsorbed with oxygen is stable under ammonia synthesis conditions(20 atm 3:1 H_2:N_2 T=673K)[39,40]. It has been shown that the addition of 0.15ML of potassium to Fe(111) and Fe(100) increases the ammonia partial dependence from -0.60 for the clean iron surfaces to - 0.35 for the 0.15ML K/Fe(111) and 0.15ML K/Fe(100) surfaces under high pressure ammonia synthesis conditions(fig. 10). The apparent order in hydrogen has been found to decrease from 0.76 for clean Fe(111) to 0.44 for the 0.15ML K/Fe(111) surface(fig.11). The Fe(110) is inactive for ammonia synthesis under these conditions with or without potassium. These changes in both the apparent order of hydrogen and ammonia occur while there is no change in the activation energy suggesting that potassium does not change the elementary steps of ammonia synthesis(fig.12). The data shows that the promotional effect of potassium is enhanced as the reaction conversion increases(i.e. increasing ammonia partial pressure).

These results agree with earlier literature[41,12] which studied the effect of potassium on doubly promoted(aluminum oxide and potassium) catalysts. It was shown that the turnover number for ammonia synthesis is roughly the same over singly(aluminum oxide) and doubly promoted iron when one atmosphere reactant pressure of nitrogen and hydrogen is used[12]. This implies that at low pressure conditions, the gas phase ammonia concentration is not high enough for potassium to exert a promoter effect. As higher reactant pressures are achieved(5 - 200atm), the promoter effect of potassium becomes significant. It was found that doubly promoted catalysts became increasingly more active than catalysts without potassium when gas phase ammonia concentration increased[41]. This implies that potassium makes the apparent order in ammonia less negative over commercial catalysts, in agreement with the single crystal work.

6.2 The Effects of Potassium on the Adsorption of Ammonia on Iron Under Ammonia Synthesis Conditions

The changes in the apparent order of ammonia suggest that to elucidate the effects of potassium, on iron single crystals and the industrial catalyst, it is necessary to understand the readsorption of gas phase ammonia on the catalyst surface during ammonia synthesis. The fact that the rate of ammonia synthesis is negative order in ammonia implies that the adsorption of gas phase ammonia product decreases the rate of ammonia synthesis. Once adsorbed the ammonia has a certain residence time(τ) on the catalyst which is determined by its adsorption energy(H_{ad}) on iron($\tau \alpha\ e^{H_{ad}/RT}$)[15]. During this residence on the catalyst, ammonia can either diffuse on the surface or decompose to atomic nitrogen and hydrogen[21,4,5]. In both cases the species produced by ammonia might reside on surface sites which would otherwise dissociatively chemisorb gas phase nitrogen, thus decreasing the rate of ammonia synthesis [2,4,5]. The promoter effect of potassium then involves lowering the adsorption energy of the adsorbed ammonia so that the concentration of adsorbed ammonia is decreased. This is supported by the temperature programmed desorption results which show that ammonia desorption from Fe(111) shifts to lower temperatures when potassium is adsorbed on the surface. Even at a 0.1ML coverage of potassium(coverage which is roughly equivalent to that stable under ammonia synthesis conditions), the adsorption energy of ammonia is decreased by 2.4kcal/mole. Thus, the residence time for the adsorbed ammonia is reduced and more of the active sites are available for the dissociation of dinitrogen. At higher coverages of potassium, the adsorption energy of ammonia decreases to an even greater extent, but these coverages could not be maintained under ammonia synthesis conditions. There also seems to be an additional adsorption site for ammonia when adsorbed on iron at high coverages of potassium as indicated by the TPD results. The development of a new desorption peak with coverages of potassium greater than 0.25ML might result from ammonia molecules interacting directly with potassium atoms;

the negative end of the ammonia dipole interacting with the potassium ion on the iron surface[36]. This interaction appears to be weak, since at a potassium coverage of 1ML, ammonia desorbs from the surface at 164 K.

Additional experimental evidence supporting the notion that ammonia blocks active sites comes from the post-reaction Auger data. Within experimental error, there is no change in the intensity of the nitrogen Auger peak between a Fe surface and a K/Fe surface after a high pressure ammonia synthesis reaction. This suggests that potassium does not change the coverage of atomic nitrogen, but instead the presence of potassium helps to inhibit the readsorption of molecular ammonia on the catalyst. High pressure reaction conditions are probably needed to stabilize this ammonia product on the iron surface at 673 K so it will not be present in the ultra-high vacuum environment. Thus, only the more strongly bound atomic nitrogen will be detected by AES in UHV.

6.3 Modeling the Kinetic Data with a Rate Equation

To model a catalytic reaction, some knowledge of the elementary reaction steps must be assumed. For ammonia synthesis it is usually accepted that the dissociative chemisorption of dinitrogen is the rate-limiting step, a process which requires two open sites on the catalyst surface[4,5]. Using Langmuir-Hinshelwood kinetics the rate of ammonia synthesis(denoted by r) can be written as

$$r = k_1 P_{N_2} \theta_v^2 \tag{1}$$

where k_1 is the rate constant for nitrogen dissociative chemisorption and θ_v is the fraction of vacant sites on the surface. It is usually assumed that atomic nitrogen is the majority species on the surface so that $\theta_v = 1 - \theta_N$ where θ_N is the fraction of surface covered by nitrogen atoms determined by the equilibrium[4];

$$N_{ad} + 1.5H_2(g) \overset{K_e}{\rightleftharpoons} NH_3(g) \tag{2}$$

where K_e is the equilibrium constant. Following the method of Langmuir θ_N can be determined and substituted into (1) so that

$$r = \frac{k_1 P_{N_2}}{[1 + (1/K_e)(P_{NH_3}/P_{H_2}^{1.5})]^2}[4]. \tag{3}$$

However, the kinetic and surface science results suggest that adsorbed ammonia blocks catalytically active sites, in addition to atomic nitrogen. In this case $\theta_v = 1 - \theta_N - \theta_{NH_3}$ where θ_N and θ_{NH_3} are determined by the equilibria

$$N_{ad} + 1.5H_2(g) \overset{K_2}{\rightleftharpoons} NH_{3ad} \tag{4}$$

and

$$NH_{3ad} \overset{K_3}{\rightleftharpoons} NH_3(g) \tag{5}$$

where K_2 and K_3 are equilibrium constants(note $K_e = K_2K_3$). Now the rate of ammonia synthesis is;

$$r = \frac{k_1 P_{N_2} P_{H_2}^3}{[P_{H_2}^{1.5} + (P_{NH_3}/K_3)(K_2^{-1} + P_{H_2}^{1.5})]^2} \tag{6}$$

The constants K_3 and K_2 can now be obtained by fitting equation 6 to the experimental data. For the clean surface, $K_3 = 0.19\text{atm}^{-1}$ and $K_2 = 2.6\times10^{-3}\text{atm}^{-1.5}$. When potassium is present, $K_3 = 0.37\text{atm}^{-1}$ and $K_2 = 2.6\times10^{-3}\text{atm}^{-1.5}$. This model, which accounts for adsorbed ammonia blocking active sites, suggests that the enhancement in ammonia synthesis rate seen over the K/Fe surfaces is due to an increase in the equilibrium constant K_3 or a shift in the equilibrium from adsorbed to gas phase ammonia. The increase in K_3 might be due to the decreased adsorption energy of ammonia when potassium is present as evidenced by the temperature programmed desorption results. The decrease in the apparent order of hydrogen is also consistent with the increase in K_3 induced by potassium. Since the rate limiting step in ammonia synthesis is the dissociation of dinitrogen, the only role of hydrogen in the rate expression(equation 6) is to create available sites for this step. In the presence of potassium, K_3 increases making more sites available as shown by the equilibria expressions (4) and (5). This is reflected in the lowering of the apparent order in hydrogen when potassium is added to the iron surface.

6.4 The Effect of Potassium on the Dissociation of Dinitrogen Under Ammonia Synthesis Conditions

Figure 13 plots the experimentally determined ratio of the clean Fe rate to the rate over K/Fe surfaces as a function of ammonia partial pressure. The ratio continuously increases as more ammonia is present in the gas phase(i.e. the promoter effect of potassium is enhanced). If the only role of potassium was to keep ammonia off the catalyst surface, then in the limit of zero ammonia partial pressure, the ratio should be unity. Instead the best fit of the model to the experimental data occurs when the ratio is 1.3 at zero ammonia partial pressure. This implies that potassium increases k_1(rate constant for dissociative dinitrogen chemisorption) by 30% on both Fe(111) and Fe(100). If the pre-exponential factor for k_1 is assumed to be the same for clean Fe and K/Fe surfaces, then a 30% increase in rate corresponds to a 0.35kcal/mole decrease in the activation energy(E_a) for this step. This change in E_a is too small to be resolved in our experiments. A small change in E_a such as this might also explain work, which was carried out on the industrial catalyst, that found the activation energy for ammonia synthesis to be only slightly higher on singly promoted(aluminum oxide) iron than it was on doubly promoted(aluminum oxide and potassium oxide) catalysts[42,12].

Enhancement of the rate limiting step in high pressure ammonia synthesis by potassium is predicted by the surface science research [43,33,27] presented earlier. It was found that elemental K on Fe increases the rate of dinitrogen chemisorption(k_1) by more than two orders of magnitude while the greatest enhancement in k_1 on Fe(111) was found to be a factor of eight[34]. The high pressure ammonia synthesis results(20atm reactant pressure and a catalyst temperature of 673K)[35], carried out on iron single crystals of (110), (100), and (110) orientations, suggest that potassium causes only about a 30% increase in k_1 on Fe(111) and Fe(100). The Fe(110) surface was found to be inactive, with or without adsorbed potassium. Under the synthesis conditions used in these studies, oxygen is needed to thermally stabilize the potassium. The presence of the oxygen might account for the small effect of potassium on k_1 in the high pressure studies since oxygen has been shown to decrease the promoter effect of potassium, at least in part, by blocking iron sites which are able to dissociatively chemisorb dinitrogen[33]. A similar effect might be expected on the industrial catalyst because it is well known that the potassium is in intimate contact with oxygen[33,38].

7 Combined Surface Science and High Pressure Studies on the Effect of Aluminum Oxide in the Ammonia Synthesis

Most early work on aluminum oxide, in relation to ammonia synthesis, suggest that the use of aluminum oxide for ammonia synthesis was simply to increase the surface area of the iron catalyst and to inhibit sintering which usually occurs with high surface area metallic particles[2,44]. This is supported by work which showed, by BET measurements, that the surface of the industrial ammonia synthesis catalyst increased ten-fold when aluminum oxide was added in the preparation phase[2]. Other workers have asserted that aluminum oxide, in addition to increasing surface area, prevents the conversion of active planes, such as Fe(111), to less active surfaces (i.e. Fe(100) and Fe(110)) during ammonia synthesis[2] but this, as of now, could not be shown because of the lack of surface structure probes in this work. Recent surface science and high pressure results will now be presented which directly investigated the iron-aluminum oxide system for ammonia synthesis over Fe(110), Fe(100), and Fe(111) model single crystal catalysts[13].

7.1 The Effects of Aluminum Oxide in Restructuring Iron Single Crystal Surfaces for Ammonia Synthesis

The initial rate of ammonia synthesis has been determined over the clean Fe(111), Fe(100), and Fe(110) surfaces with and without aluminum oxide. The addition of aluminum oxide to the (110), (100), and (111) faces of iron decreases the rate of ammonia synthesis in direct proportion to the amount of surface covered[39]. This suggests that the promoter effect of aluminum oxide involves intimate contact with the iron which can not be achieved by simply depositing aluminum oxide on an iron catalyst.

Remembering that the industrial catalyst is prepared by fusing 2-3% by weight of aluminum oxide and potassium with oxidized iron(Fe_3O_4), experiments were performed in which Al_xO_y/Fe single crystal surfaces were pretreated in an oxidizing environment prior to ammonia synthesis. These experiments were carried out by depositing about 2ML of Al_xO_y on Fe(111), Fe(100), and Fe(110) surfaces and then treating them in varying amounts of water vapor in order to oxidize the iron and to induce an interaction between iron oxide and aluminum oxide. After removing the water vapor, high pressures of nitrogen and hydrogen were added to determine rates of ammonia synthesis. Figure 14 shows the rate of ammonia synthesis over Al_xO_y/Fe surfaces which have been pretreated with water vapor prior to ammonia synthesis. The initially inactive Al_xO_y/Fe(110) surface restructures and becomes as active as the Fe(100) surface after a 0.05 Torr water vapor treatment and as active as the Fe(111) surface after a 20 Torr water vapor pretreatment. This is about a 400-fold increase in the rate of ammonia synthesis over clean Fe(110)[16]. The activity of the Al_xO_y/Fe(100) surface can also be enhanced to that of the highly active Fe(111) surface by utilizing a 20 Torr water vapor pretreatment and this high activity is maintained for over four hours as in the case for the restructured Al_xO_y/Fe(110). Little change in the activity of the Fe(111) surface is experimentally seen when it is treated in water vapor in the presence of Al_xO_y.

The activity of the Fe(110) and Fe(100) surfaces for ammonia synthesis can also be enhanced to the level of Fe(111) by water vapor pretreatments in the *absence* of aluminum oxide but in this circumstance the enhancement in activity is only transient. Figure 15 shows the rate of ammonia synthesis as a function of reaction time for a restructured Fe(110) and Al_xO_y/Fe(110) surfaces. Both surfaces have an initial activity similar to the clean Fe(111) surface. The restructured Al_xO_y/Fe(110) surface maintains this activity for over four hours while the restructured Fe(110) surface loses it activity for ammonia synthesis within one hour of reaction.

7.2 Characterization of the Restructured Surfaces

For the Al_xO_y/Fe(110) and Al_xO_y/Fe(100) to become as active as the Fe(111) surface for ammonia synthesis there seems to be new crystal orientations being created upon restructuring the Al_xO_y/Fe(110) and Al_xO_y/Fe(100) surfaces in water vapor. An increase in the surface area does not account for the enhancement in rate since it has been shown that about 40% less carbon monoxide adsorbs on restructured Al_xO_y/Fe(110) and Al_xO_y/Fe(100) relative to the clean respective surfaces[13].

Auger electron spectroscopy, low energy electron diffraction, temperature programmed desorption, and scanning electron microscopy(SEM) have been used to characterize the restructured surfaces. SEM micrographs for restructured Fe(110) and Al_xO_y/Fe(110) surfaces are shown in figures 16 and 17 respectively. The Al_xO_y/Fe(110) surface, restructured with 0.05 Torr of water vapor(fig.16a) shows features about 1μm across growing on the Fe(110) substrate(the clean Fe(110) surface is smooth and featureless). After a 20 Torr water vapor pretreatment the surface seems to be completely restructured with features covering the whole surface(fig. 16b). Auger electron spectroscopy finds that only about 5% of the iron surface is covered by aluminum oxide. Sputtering the surface with argon ions reveals aluminum oxide beneath the iron surface.

SEM micrographs of restructured Fe(110) shows none of the features associated with the restructured Al_xO_y/Fe(110) surface. Figure 17a shows a (110) surface which has been restructured with 20 Torr of water vapor. No LEED pattern is obtainable from this surface. Its appearance is different than the restructured iron single crystals which had aluminum oxide present. None of the crystallite structures associated with the restructured Al_xO_y/Fe(110) surface are present. Figure 17b shows the restructured Fe(110) surface after one hour of ammonia synthesis. The features are now gone and the surface has no activity towards ammonia synthesis. In addition, it exhibits a (1×1)LEED pattern representative of clean Fe(110).

Ammonia temperature programmed desorption from iron single crystal surfaces after high pressure ammonia synthesis proves to be a sensitive probe of the new surface binding sites formed upon restructuring. Ammonia TPD spectra for the four surfaces are shown in Figure 18. Each surface shows distinct desorption sites. The Fe(110) surface displays one desorption peak (β_3) with a peak maximum at 658K. Two desorption peaks are seen for the Fe(100) surface (β_2 and β_3) at 556K and 661K. The Fe(111) surface exhibits three desorption peaks (β_1, β_2, and β_3) with peak maxima at 495K, 568K, and 676K, and the Fe(211) plane has two desorption peaks (β_2 and β_3) at 57OK and 676K. Temperature programmed desorption spectra for the Al_xO_y/Fe(110), Al_xO_y/Fe(100), and Al_xO_y/Fe(111) surfaces restructured in 20 Torr of water vapor are shown in Figure 19. A new desorption peak, β_2 develops on the restructured Al_xO_y/Fe(110) surface, and an increase in the β_2 peak occurs on the restructured Al_xO_y/Fe(100) surface. The β_2 peaks from the restructured Al_xO_y/Fe(110) and Al_xO_y/Fe(100) surfaces grow in the same temperature range as the Fe(111) and Fe(211) β_2 peaks. Deactivation of the restructured surfaces by prolonged sputtering at 832K reduces the intensity of the β_2 peaks on the restructured Al_xO_y/Fe(110) and Al_xO_y/Fe(100) surfaces to the same level as the respective clean surfaces.

The clean Fe(110), Fe(100), and Fe(111) surfaces restructured with 20 Torr of water vapor produce the same TPD spectra as the Al_xO_y restructured surfaces. Deactivation of the (100) and (110) clean restructured iron surfaces is quick under the ammonia synthesis conditions and the β_2 peaks become equivalent in intensity to those on the respective clean surfaces within one hour of ammonia synthesis.

The nature of restructuring of the Al_xO_y/Fe surfaces is indicated by the kinetic and TPD results. Kinetic data shows that through restructuring the activity towards ammonia synthesis of the Fe(110) and Fe(100) planes approaches that of the clean Fe(111) or Fe(211) planes while the Fe(111) plane is not affected greatly by restructuring. The activity of the clean Fe(111) and Fe(211) planes is usually attributed to the presence of C_7 sites (see section 4). The clean Fe(100) and Fe(110) plane lack these sites. This suggests that restructuring in water vapor produces highly coordinated C_7 sites on the restructured Fe(110) and Fe(100) surfaces. The increase in rates over the restructured Fe(110) and Fe(100) planes is not attributable to an increase in surface area since less CO is adsorbed on these surfaces when compared to the respective clean surfaces. A similar decrease in CO adsorption has also been observed on MgO/Fe ammonia synthesis catalysts that have been restructured with ammonia[45](see section 4). These results were interpreted as due to the formation of C_7 sites which are not able to adsorb as much CO as lower coordinated sites because of steric reasons. This explanation is applicable to the present study and it further supports the idea of formation of C_7 sites upon water vapor restructuring.

The ammonia TPD results point towards the formation of surface orientations which contain C_7 sites during water vapor induced restructuring. The growth of the β_2 peaks upon restructuring of the Fe(110) and Fe(100) surfaces suggests that the surfaces change orientation upon water vapor treatment. The β_2 peaks also reside in the same temperature range as the Fe(111) β_2 peak. It seems likely that the TPD peaks in this temperature range act as a signature for the C_7 site since the Fe(211) surface (fig.10), which contains C_7 sites and is highly active in the ammonia synthesis reaction, also exhibits a β_2 peak after ammonia synthesis with a peak maximum at 57OK. These results suggest that surface orientations which contain C_7 sites, such as the Fe(111) and Fe(211) planes, are being formed during the reconstruction of clean and Al_xO_y treated iron surfaces, but only in the presence of Al_xO_y does the active restructured surface remain stable under the ammonia synthesis conditions.

7.3 The Restructuring of Iron by Aluminum Oxide

The process by which iron restructures seems to involve both oxidation and reduction. Initial oxidation by water vapor destroys the original morphology of the iron surface. On reduction with nitrogen and hydrogen, the oxygen is removed and the resulting metallic iron is left in orientations active for the ammonia synthesis, such as Fe(111) and Fe(211). The presence of an amorphous surface after water vapor pretreatment can not be ruled out, since by using the industrial catalyst[46] it was shown by in-situ x-ray diffraction at high pressures that the catalyst surface is amorphous with no discernable crystal structure. Even if the surface is amorphous the important point is that C_7 sites are present and if no support phase is present (i.e. Al_xO_y), reconversion of the iron into less active orientations is rapid under ammonia synthesis conditions. The idea of aluminum oxide stabilizing active planes for ammonia synthesis can be seen in the literature[2] but this work is the first direct experimental proof substantiating this claim.

With the addition of Al_xO_y, the mobility of the iron is increased and restructuring can occur at lower pressure of water vapor. The SEM micrographs suggest that iron is forming crystallites on top of the restructured Al_xO_y/Fe(110) surface (opposed to the uniform appearance of the restructured clean Fe(110) surface). AES finds little Al_xO_y on the surface, suggesting that the iron has diffused on top of the Al_xO_y islands. These findings can be explained by considering wetting properties and the minimization of the free energy for the iron oxide-aluminum oxide system.

In vacuum or in a reducing environment (i.e. ammonia synthesis conditions), metallic iron will not spread over aluminum oxide (metallic iron has a higher surface tension than aluminum oxide [47]). Conversely, in an oxidizing environment (i.e. the water vapor treatments) iron oxide forms (the surface tension of the oxide will be lower than the metal [47,48]) and a chemical interaction between iron and aluminum oxide might result as inferred from AES results[13] shown in figure 20. It is shown that the 42eV Auger peak representative of iron oxide[49,50] is shifted to about 38eV in the presence of aluminum oxide and water vapor, indicating that an interaction results between aluminum oxide and iron oxide. Both these considerations favor iron wetting the aluminum oxide. Using transmission electron microscopy, it has been shown that iron wets alumina (Al_2O_3) in an oxidizing environment or even in the presence of hydrogen which contains trace amounts of water vapor [51]. Using micro-electron diffraction, the formation of iron aluminate (i.e. $FeAl_2O_4$) in the presence of an oxygen source was also postulated [51].

Whereas 20 Torr of water vapor was needed to restructure clean iron single crystals, only 0.4 Torr of water vapor is needed to restructure an Al_xO_y/Fe surface. It seems that Al_xO_y provides an alternate and apparently more facile mechanism for the migration of iron. Upon reduction, metallic iron is left in a highly active orientation (such as Fe(111) and Fe(211)) for the ammonia synthesis reaction. The Al_xO_y now stabilizes the active iron, since if the Al_xO_y were not present the iron would move to positions coincident with the bulk periodicity(see figure 21 for a schematic representation of the restructuring).

The formation of an iron aluminate during reconstruction of the iron surface may be responsible for the stability of the restructured Al_xO_y/Fe surfaces. The formation of iron aluminate has been postulated in XPS studies on Fe-Al_2O_3 and Fe_3O_4-Al_2O_3 systems [52,53] as well as in numerous studies on the industrial ammonia synthesis catalyst [54,55,56]. The volume of an $FeAl_2O_4$ molecule is approximately equal to the volume of seven iron atoms in a bcc lattice [54] so that $FeAl_2O_4$ can exist as a skeleton in the iron lattice with little distortion. The low coverages of Al_xO_y on the restructured surfaces suggest that the support effect might be coming through inclusions of $FeAl_2O_4$ in the near surface region. This is supported by the fact that ion sputtering the restructured surfaces reveal subsurface Al_xO_y.

8 Combined UHV/High Pressure Studies on the Interaction Between Aluminum Oxide and Potassium Coadsorbed on Iron

The industrial catalyst employed for use in ammonia synthesis usually contains both aluminum oxide and potassium. Surface science and catalytic studies will be presented which study the interactions between the two promoters[40].

8.1 The Stability of Potassium on Iron when Coadsorbed with Aluminum Oxide

Figure 22 shows Auger spectra of a K/Fe(100) surface prepared prior to carrying out ammonia synthesis, a K/Fe(100) surface after reaction, and a post-reaction K/40%Al_xO_y/Fe(100) surface. It is apparent that the surface with aluminum oxide can retain more potassium during ammonia synthesis conditions than the surface without aluminum oxide. This suggests that aluminum oxide binds directly to potassium or there is an interaction mediated through the iron surface. To probe these interactions experiments were performed in which a known amount of Al_xO_y was deposited on a Fe(100) surface. About 1ML of potassium was evaporated on the crystal and the sample was heated to 673K in UHV. The potassium Auger signal was monitored periodically. A rapid decrease occurs in the potassium Auger signal initially which is due to the low desorption energy of potassium at high coverages. After about 20 minutes a steady state concentration of potassium is established. The final coverage of potassium is approximately equal to the initial coverage of aluminum oxide. This result is represented in figure 23 where the relative concentration of stabilized potassium is plotted against the relative concentration of stabilized potassium. An approximate 1:1 ratio is found between the surface concentration of potassium and aluminum oxide, and this is suggestive of compound formation between the two additives(i.e. $KAlO_2$), as opposed to a non-stoichiometric Al_xO_y-K surface layer[39].

8.2 The Effects of Coadsorbed Potassium and Aluminum Oxide on the Ammonia Synthesis Over *Unrestructured* Fe(100)

Figure 24 shows the rate of ammonia synthesis versus % free iron surface, as determined by carbon monoxide TPD(see experimental section). The rate of ammonia synthesis decreases roughly in proportion to the amount of iron covered by the aluminum oxide and potassium[39]. Only site-blocking is occurring at initial reaction conversions (P_{NH_3} ranges from 0 to 3 Torr during this measurement).

As the reaction conversion increases, the effects of coadsorbed potassium and aluminum oxide become apparent[40]. Figure 25 plots the ammonia partial pressure in the reactor loop versus time for the 0.15 ML K/Fe(100), clean Fe(100), 0.25ML K/25% Al_xO_y/Fe(100) and for the 25% Al_xO_y surfaces. In these experiments about 10-13 Torr of ammonia was introduced into the reactor loop prior to ammonia synthesis. The 0.25ML K/25% Al_xO_y/Fe(100) surface becomes increasingly more active than the 25% Al_xO_y/Fe(100) surface as the reaction conversion increases. This is the same behavior which is observed when the activity of 0.15ML K/Fe(100) is compared to Fe(100)(see section 6). The presence of potassium on the iron surface reduces the adsorption energy of the ammonia product. Thus, the concentration of surface ammonia is lowered and more catalytic sites are available for the dissociation of dinitrogen. Frankenburg[3], has suggested that on the industrial catalyst, potassium neutralizes weak acidic sites which would otherwise bind ammonia and ammonia decomposition products. This type of promotion might be an additional effect of potassium when coadsorbed with aluminum oxide although detailed experiments have not been carried out to address this possibility.

Even though more potassium can be stabilized on the iron surface when aluminum oxide is coadsorbed, an enhancement in the promoter effect was not found when these surfaces were compared to the activity of 0.15ML K/Fe(100). The 0.25ML K/25% Al_xO_y/Fe(100) surfaces exhibits roughly the same rate as the 0.15ML K/Fe(100) surface, as indicated by the slopes of the curves in figure 25. The surface area of the single crystal and the fraction of surface covered by the additive is taken into account when the rates of ammonia synthesis are determined. Thus, the potassium, which interacts with the aluminum oxide, seems to be rendered catalytically inactive. Stabilizing more than 0.25ML of potassium actually decreases the promoter effect of potassium. This decrease is probably due to high coverages of potassium blocking catalytic sites which dissociate dinitrogen[39].

8.3 Water Vapor Pretreatment of Clean and Al_xO_y/Fe Single Crystal Surfaces in the Presence of Coadsorbed Potassium

Coverages of 0.1 to 1.0 ML of potassium adsorbed alone on the (111), (100), and (110) faces of iron failed to produce any promotional effects after pretreatments of 0.05, 0.4, and 20 Torr of water vapor (after the water vapor treatments the coverage of potassium was never more than 0.4 ML and it did not exceed 0.1 ML after the ammonia synthesis reaction in agreement with previous work[39]).

The same coverages of potassium coadsorbed with two monolayers of aluminum oxide on the Fe(110), Fe(100), and Fe(111) surfaces hindered the restructuring process in water vapor(see section 7). As increasing amounts of potassium were coadsorbed, more aluminum oxide was detected by AES after water pretreatments of 20 Torr, and less restructuring of the iron occurred (rates of ammonia synthesis over these surfaces were less than those surfaces which were restructured with just aluminum oxide). There is a one to one ratio between aluminum oxide and potassium on the surface and in a case where one monolayer of potassium was deposited on two monolayers of aluminum oxide, AES showed that no aluminum oxide or potassium left the iron surface after a 20 Torr water vapor pretreatment and restructuring failed to occur.

8.4 The Effects of Coadsorbed Potassium and Aluminum Oxide on the Ammonia synthesis Over *Restructured* Fe(100)

It has been shown that inactive Fe(110) and the little active Fe(100) surface can be restructured with water vapor in the presence of aluminum oxide to produce new surfaces as active as Fe(111) and Fe(211). The coadsorption of potassium with the aluminum oxide inhibits this restructuring. It seems likely that the formation of an potassium aluminate retards the interaction between aluminum oxide and iron which is needed to change the iron surface morphology. Thus, the promotional effect of both aluminum oxide and potassium is eliminated if they are added together prior to the restructuring process.

To fully realize the promotional effects of potassium and aluminum oxide the promoters must be added at different times during the preparation of the active catalyst[40]. Figure 26 plots the ammonia partial pressure in the reaction loop versus the time of reaction for clean Fe(100), restructured Al_xO_y/Fe(100) and restructured 0.25ML K/25% Al_xO_y/Fe(100) where the potassium was added after the restructuring procedure(see figure for conditions). The restructured Al_xO_y/Fe(100) surface with 0.25% Al_xO_y is about one order of magnitude more active than the clean Fe(100) surface when the surface areas of the samples are taken into account. The addition of 0.25ML K to a restructured Al_xO_y/Fe(100) surface increases the activity of the restructured surface twofold at an ammonia partial pressure of 20 Torr. Thus the restructured 0.25ML K/25% Al_xO_y/Fe(100) surface is now 20 times more active than the clean Fe(100) surface. The only way to achieve this much enhancement is to restructure the surface in the presence of only aluminum oxide, and then to add the potassium.

9 Summary of the Promoter Effects of Potassium and Aluminum Oxide

This chapter summarizes surface science and catalytic studies on the promoter effects of both aluminum oxide and potassium for ammonia synthesis over iron single crystal surfaces. The promoter effect of potassium on ammonia synthesis has been investigated over the Fe(110), Fe(100), and Fe(111) surfaces under high pressure conditions. A coverage of 0.15ML is the maximum amount of potassium that can be stabilized on the iron single crystals under ammonia synthesis conditions. Adsorbed potassium has no promotional effect on the inactive Fe(110) surface. However, adsorbed potassium increases the rate of ammonia synthesis markedly over the Fe(111) and Fe(100) crystal faces. The promotional effect becomes enhanced as the reaction conversion increases. For example, at an ammonia partial pressure of 20 Torr there is a two-fold increase in the rate of ammonia synthesis over Fe(111) and Fe(100) in the presence of potassium. The presence of potassium changes the ammonia reaction order from -0.6 to -0.35 on the (100) and (111) faces of iron. Adsorbed potassium decreases the reaction order in hydrogen from 0.76 to 0.44 on Fe(111). However, within experimental error, there is no change in the activation energy, when potassium is present, suggesting that the mechanism for ammonia synthesis in not being changed.

The kinetic data is explained by a model which accounts for the blocking of catalytic sites, which have the ability to dissociate dinitrogen, by adsorbed ammonia and atomic nitrogen. The presence of potassium lowers the concentration of adsorbed ammonia on the surface, making more sites available to dissociatively chemisorb dinitrogen, further increasing the rate of ammonia synthesis. The model suggests that an additional promoter effect by potassium is a 30% enhancement of the rate of dinitrogen dissociation on Fe(111) and Fe(100), further increasing the rate of ammonia production. This is in qualitative agreement with nitrogen chemisorption studies on Fe and K/Fe surfaces in UHV(section 5).

Treating the (110), (100), and (111) faces of iron with 20 Torr of water vapor causes surface restructuring. The restructured Fe(110) and Fe(100) surfaces become as active as the clean Fe(111) surface for ammonia synthesis. The restructured Fe(111) exhibits a slight decrease (about 5%) in activity when compared to the clean Fe(111) surface. The restructured (110), (100), and (111) surfaces reconvert to their unrestructured orientations within one hour of ammonia synthesis.

The same restructuring on the Fe(110), Fe(100), and Fe(111) surfaces can be performed with water vapor in the presence of aluminum oxide. In this case, 20 Torr of water vapor restructures the Al_xO_y/Fe(100) and only 0.4 Torr of water vapor is needed to restructure the Al_xO_y/Fe(110) surface so that they become as active as the Fe(111) face in ammonia synthesis. The restructured Al_xO_y/Fe(110) and Al_xO_y/Fe(100) surfaces maintain their activity for longer than four hours in the ammonia synthesis conditions. The formation of iron aluminate in the iron near surface region is invoked to explain the stability of the restructured Al_xO_y/Fe surfaces.

The reaction rate studies and ammonia temperature programmed desorption results suggest that planes containing C_7 sites, such as the Fe(211) and Fe(111) surfaces, are being created during the water vapor pretreatments with or without aluminum oxide. Only when aluminum oxide is present will these active surfaces remain stable and not reconvert to less active surfaces (i.e. Fe(11O) and Fe(1OO) planes).

The coadsorption of potassium with the aluminum oxide inhibits the restructuring process. Thus, to realize the full promotional effects of aluminum oxide and potassium the surfaces should be restructured with only aluminum oxide and potassium should be added afterwards. Using this procedure, the activity of the Fe(110) surface can be increased by a factor of about 800 at an ammonia partial pressure of 20 Torr(P_{N_2}=5atm and P_{H_2}=15atm). Restructuring leads to about a 400 fold increase in the activity of Fe(110), and adding potassium contributes a two-fold increase in addition to this.

The application of these results to the industrial catalyst seems to be warranted. The industrial catalyst is prepared by fusing 1-3% by weight of aluminum oxide and potassium to iron oxide with subsequent reduction to the active catalyst in a stoichiometric mixture of nitrogen and hydrogen. This procedure has been reproduced in the combined UHV / high pressure studies presented in this chapter. The promoter effect of aluminum oxide in the industrial catalyst results from its interaction with the iron oxide during the preparation stage. This interaction probably results in an iron aluminate, and this prevents planes such as Fe(111) and Fe(211), formed during reduction, from converting to more thermodynamically stable planes such as the little active Fe(110) and Fe(100) surfaces. The presence of potassium seems to have little to do with this structural promotion. Actually, its presence during this step might inhibit the full promotional effect of aluminum oxide from being realized. Its interaction with aluminum oxide seems to form a potassium aluminate which retards the interaction between iron oxide and aluminum oxide during the restructuring process.

Acknowledgement

This work was supported by the Director, Office of Energy Research, Office of Basic Energy Sciences, Materials Science Division of the U.S. Department of Energy under contract number DE-AC03-76SF00098. The authors gratefully acknowledge partial support for this research by I.C.I. The authors also thank Sabrina Fu for carefully proofreading the manuscript.

References

[1] A. Nielsen. *An Investigation on promoted Iron Catalysts for the Synthesis of Ammonia.* Jul. Gjellerups Forlag, 3rd Ed., Copenhagen, 1968.

[2] A. Ozaki. *Catalysis, Science and Technology*, chapter 3. Volume 1, Springer-Verlag, Berlin, 1981.

[3] W.G Frankenburg. Catalysis. page 171, Reinhold, New York, 1955.

[4] M. Temkin and V. Pyzhev. *Acta Phys. Chim. URSS* **12** (1940) 327.

[5] A. Ozaki, H.S. Taylor, and M. Boudart. *Proc. Roy. Soc. (London)* **47** (1960) 258.

[6] S.A. Topham. *Catalysis, Science and Technology.* Volume 7, Springer-Verlag, Berlin, 1985.

[7] G. Ertl. *J. Vac. Sci. Technol. A* **1(2)** (1983) 1247.

[8] S. Brunauer and P.H. Emmett. *J. Amer. Chem. Soc.* **62** (1940) 1732.

[9] R. Krabetz and C. Peters. *J. Amer Chem. Soc.* **77** (1965) 333.

[10] P.H. Emmett and S. Brunauer. *J. Amer. Chem. Soc.* **59** (1937) 310.

[11] H.H. Madden and W. Goodman. *Surface Sci.* **150** (1985) 39.

[12] S. Khammouma. PhD thesis, Stanford Univ., 1972.

[13] D.R. Strongin, S.R. Bare, and G.A. Somorjai. *J. Catal.* **103** (1987) 289.

[14] D.W. Blakely, C.I. Kozak, B.A. Sexton, and G.A. Somorjai. *J. Vac. Sci. Tech.* **13** (1976) 1091.

[15] G.A. Somorjai. *Chemistry in Two Dimensions: Surfaces.* Cornell University Press, Ithaca, 1981.

[16] N.D. Spencer, R.C. Schoonmaker, and G.A. Somorjai. *J. Catal.* **74** (1982) 129.

[17] D.R. Strongin, J. Carrazza, S.R. Bare, and G.A. Somorjai. *J. Catal.* **103** (1987) 213.

[18] R. Smoluchoswki. *Phys. Rev.* **60** (1941) 661.

[19] J. Hoelzl and F.K. Schulte. *Solid Surface Physics.* Springer-Verlag, 1979.

[20] J. McAllister and R.S. Hansen. *J. Chem. Phys.* **59** (1973) 414.

[21] G. Ertl. Robert welch conferences on chemical research xxv heterogeneous catalysis. In *Catalysis Reviews*, page 179, Houston, 1981.

[22] A. Nielsen. *Catal. Rev.* **4** (1970) 1.

[23] L. Falicov and G.A. Somorjai. *Proc. Nat. Acad. Sci. USA* **82** (1985) 2207.

[24] J.A. Dumesic, H. Topsøe, and M. Boudart. *J. Catal.* **37** (1975) 513.

[25] M. Asscher, J. Carrazza, M.M. Khan, K.B. Lewis, and G.A. Somorjai. *J. Catal.* **98** (1986) 227.

[26] G. Broden and H. P. Bonzel. *Surf. Sci.* **84** (1979) 106.

[27] S.B. Lee, M. Weiss, and G. Ertl. *Surf. Sci.* **108** (1981) 357.

[28] R.L. Gerlach and T.N. Rhodin. *Surf. Sci.* **19** (1970) 403.

[29] P.H. Redhead. *Vacuum* **12** (1962) 203.

[30] G. Pirug, G. Broden, and H.P. Bonzel. *Surf. Sci.* **94** (1980) 323.

[31] F. Bozso, G. Ertl, M. Grunze, and M. Weiss. *J. Catal.* **49** (1977) 18.

[32] F. Bozso, G. Ertl, M., and M. Weiss. *J. catal.* **50** (1977) 519.

[33] Z. Paal, G. Ertl, and S.B. Lee. *Appl. Surf. Sci.* **8** (1981) 231.

[34] G. Ertl, S.B. Lee, and M. Weiss. *Surf. Sci.* **114** (1982) 527.

[35] D.R. Strongin and G.A. Somorjai. *submitted to J. Catal.* () .

[36] T.E. Madey and C. Benndorf. *Surf. Sci.* **152/153** (1985) 587.

[37] C. Benndorf and T.E. Madey. *Chem. Phys. Letters* **101** (1983) L277.

[38] J.G. van Ommen, W.J. Bolink, J. Prasad, and P. Mars. *J. Catal.* **38** (1975) 120.

[39] S.R. Bare, D.R. Strongin, and G.A. Somorjai. *J. Phys. Chem.* **90** (1986) 4726.

[40] D.R. Strongin and G.A. Somorjai. *submitted to J. Catal.* () .

[41] K. Altenburg, H. Bosch, J.G. Ommen, and P.J. Gellings. *J. Catal.* **66** (1980) 326.

[42] R. Brill. *J. Pol. Sci.* **12** (1962) 353.

[43] G. Ertl, M. Weiss, and S.B. Lee. *Chem. Phys. Lett.* **60** (1979) 391.

[44] W.D. Mross. *Catal. Rev. -Sci. Eng.* **25(4)** (1983) 591.

[45] J.A. Dumesic, H. Topsøe, and M Boudart. *J. Catal.* **37** (1975) 513.

[46] T. Rayment, R. Schlogl, J.M. Thomas, and G. Ertl. *Nature* **315** (1985) 311.

[47] S.H. Overbury, P.A. Bertrand, and G.A. Somorjai. *Chem. Rev.* **75(5)** (1975) 547.

[48] Oxides and oxide films. In Ashok k. Vijh, editor, , Deckker, New York, 1981.

[49] M. Langell and G.A. Somorjai. *J. Vac. Sci. and Tech.* **21** (1982) 858.

[50] G. Ertl and K. Wandelt. *Surface Sci.* **50** (1975) 479.

[51] I. Sushumna and E. Ruckenstein. *J. Catal.* **94** (1985) 239.

[52] E. Paparazzo, J.L. Dormann, and D. Fiorani. *Phys. Rev. B* **28** (1983) 1154.

[53] E. Paparazzo. *Appl. Surf. Sci.* **25** (1986) 1.

[54] W.S. Borghard and M. Boudart. *J. Catal.* **80** (1983) 194.

[55] H. Ludwiczek, A. Preisinger, A. Fischer, R. Hosemann, A. Schonfeld, and W. Vogel. *J. Catal.* **51** (1978) 326.

[56] Fagherazzi G., F. Galante, F. Garbassi, and N. Pernicone. *J. Catal.* **26** (1972) 344.

[57] Z. Paal, G. Ertl, and S.B. Lee. *Appl. Surface Sci.* **8** (1981) 231.

10 Figure Captions

Figure 1. The rate of ammonia synthesis over the five iron surfaces studied exhibiting the structure sensitivity of ammonia synthesis[17].

Figure 2. Schematic representations of the (111), (210), (100), (211), and (110) orientations of iron[17]. The coordination for each surface atom is indicated.

Figure 3. The structure sensitivity of ammonia synthesis over rhenium single crystal surfaces[25]. Schematics of the atomic structure of each surface is given above each bar.

Figure 4. TPD spectra[33] for potassium adsorbed on a polycrystalline Fe surface suggest that potassium will not be stable under stationary ammonia synthesis conditions($T \approx 673$ K).

Figure 5. The presence of oxygen thermally stabilizes potassium[33] (a) $n_K = 2.45\times10^{14}\mathrm{cm}^{-2}$; (b) $n_K = 2.06\times10^{14}\mathrm{cm}^{-2}$, $Y_0 = 0.90$(O adsorbed first); (c) $n_K = 2.61\times10^{14}\mathrm{cm}^{-2}$, $Y_0 = 0.62$(K adsorbed first). Y_0 is defined as the ratio between the oxygen Auger intensity and iron Auger intensity($Y_0 = \frac{I_{O(510eV)}}{I_{Fe(650eV)}}$).

Figure 6. The variation of σ_0 with the addition of potassium[34] to Fe(100) at 430 K. σ_0 can be enhanced by a factor of 280 relative to clean Fe(100).

Figure 7. σ_0 as a function of potassium coverage on Fe(111) at 430 K[34]. σ_0 can be enhanced by a factor of 8 in the presence of potassium.

Figure 8. The effect of oxygen on $\sigma_0(=\frac{S_0}{10^5})$ for a K/Fe(polycrystalline) surface[33]. The decrease in σ_0 is attributed to the physical blockage of surface sites by oxygen. Y_0 is defined as the ratio between the oxygen Auger intensity and iron Auger

intensity($Y_0 = \frac{I_{O(510eV)}}{I_{Fe(650eV)}}$).

Figure 9. Ammonia temperature programmed desorption from Fe(111) and K/Fe(111)[35]. The desorption temperature of ammonia from Fe(111) is lowered in the presence of potassium. Thus potassium lowers the adsorption energy of ammonia on the iron surface.

Figure 10. The apparent order in ammonia for ammonia synthesis over Fe(100) and K/Fe(100) surfaces[35]. The order in ammonia becomes less negative when potassium is present. The same values, within experimental error are found for the Fe(111) and K/Fe(111) surfaces.

Figure 11. The apparent reaction order in hydrogen for ammonia synthesis over Fe(111) and K/Fe(111) surfaces[35]. The order in hydrogen decreases in the presence of potassium.

Figure 12. The activation energy(E_a) for Fe(111) and K/Fe(111)[35]. Within experimental error there is no change in E_a suggesting that potassium does not change the fundamental reaction steps of ammonia synthesis.

Figure 13. The experimental fit of reaction rates over Fe and K/Fe surfaces to a model which allows for the blocking of catalytic sites by adsorbed ammonia as well as atomic nitrogen[35]. In the presence of potassium K_3 is increased.

Figure 14. Rates of ammonia synthesis over clean iron single crystals and restructured Al_xO_y/Fe surfaces[13]. Restructuring conditions are given in the figure.

Figure 15. Deactivation of the restructured Fe(110) surface occurs within one hour while the restructured Al_xO_y/Fe(110) surface maintains its activity for greater than four hours under ammonia synthesis conditions[13].

Figure 16. SEM of the restructured Al_xO_y/Fe(110) surface[13]. (a)after a 0.05 Torr water vapor treatment and reduction in nitrogen and hydrogen. (b) after a 20 Torr water vapor pretreatment followed by reduction. The aluminum oxide is located underneath the iron surface so it does not block active catalytic iron sites.

Figure 17. SEM of the restructured Fe(110) surface[13]. (a) after a 20 Torr pretreatment in water vapor and (b) after one hour of ammonia synthesis. Note that the features smooth out under ammonia synthesis conditions.

Figure 18. Ammonia TPD after high pressure ammonia synthesis[13]. The low temperature peaks exhibited by Fe(111) and Fe(211) (β_1 and β_2) are attributed to the presence of C_7 sites.

Figure 19. Ammonia TPD after ammonia synthesis from restructured Al_xO_y/Fe surfaces[13]. The restructured Al_xO_y/Fe(110) and Al_xO_y/Fe(100) surfaces exhibit low temperature peaks similar to Fe(111) and Fe(211). Thus, restructuring by water vapor creates active C_7 sites.

Figure 20. AES spectra of oxidized iron and a partially oxidized iron-aluminum oxide surface[13]. The 42eV iron peak shifts to 39eV in the presence of aluminum oxide.

Figure 21. A schematic depicting the restructuring process of iron, induced by water vapor, and in the presence of aluminum oxide. The oxidation of the iron allows iron oxide to migrate on top of aluminum oxide. An interaction between the aluminum oxide and iron oxide might enhance this step. Upon reduction in nitrogen and hydrogen the iron is left in active and stable orientations for ammonia synthesis. The formation of iron aluminate might be responsible for this stability.

Figure 22. AES spectra of promoted Fe(100) surfaces before and after ammonia synthesis[39]. The pre-reaction potassium signal corresponds to 1ML.

Figure 23. The relative concentration of stabilized potassium plotted against the relative concentration of aluminum oxide present[39]. The dotted line corresponds to a 1:1 ratio of potassium to aluminum oxide.

Figure 24. The rate of ammonia synthesis decreases roughly in proportion to the amount of iron covered by potassium and aluminum oxide at initial reaction conversions[39].

Figure 25. The amount of ammonia produced in the reaction loop is plotted against time of ammonia synthesis for the 0.15ML K/Fe(100), clean Fe(100), 0.25ML K/25% Al_xO_y/Fe(100), and 25% Al_xO_y/Fe(100) surfaces[40]. The non-linearity of the curves is due to gas phase ammonia readsorbing on the catalyst and blocking catalytic sites for the dissociation of dinitrogen.

Figure 26. Ammonia accumulation in the reaction loop is plotted against time for the clean Fe(100), restructured Al_xO_y/Fe(100) and for a 0.25ML K/Al_xO_y/Fe(100) which had been restructured before the addition of potassium[57].

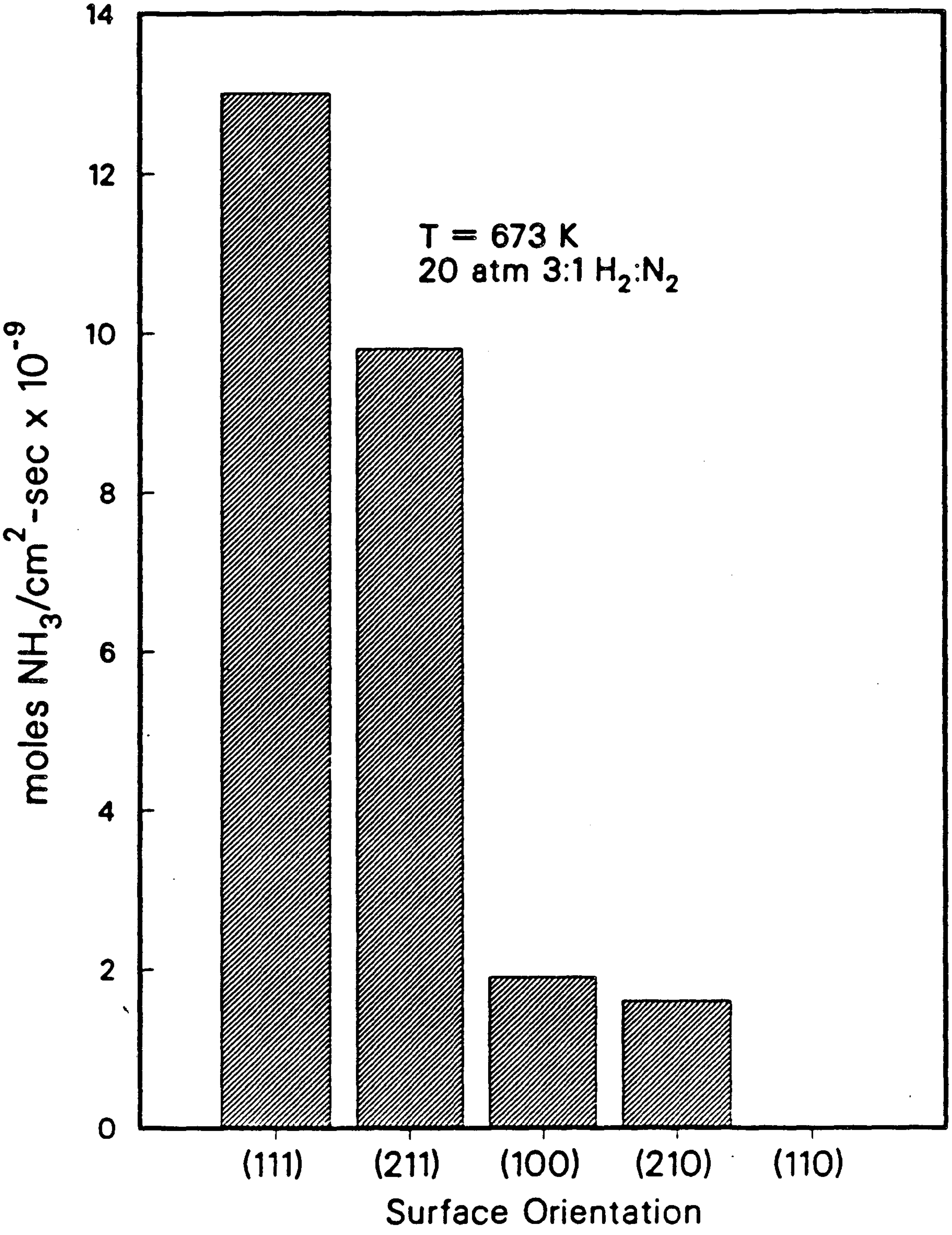
14
12
10
8
6
4
2
0
moles NH_3/cm^2-sec x 10^{-9}
T = 673 K
20 atm 3:1 H_2:N_2
(111)
(211)
(100)
(210)
(110)
Surface Orientation

XBL 864-1663

Fe(111)

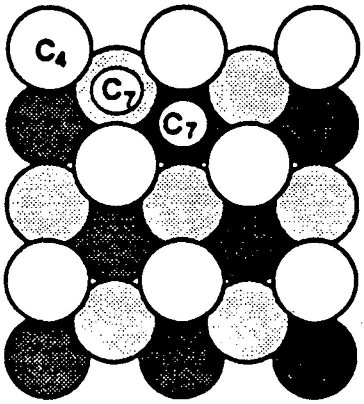

Fe(210)

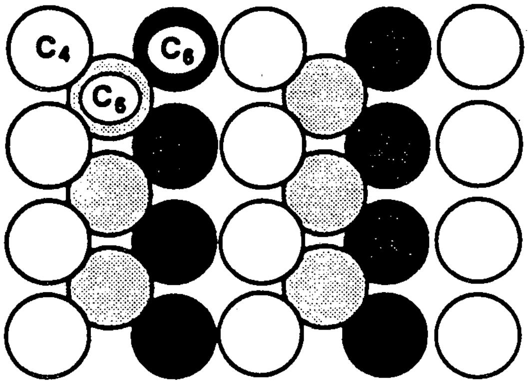

Fe(100)

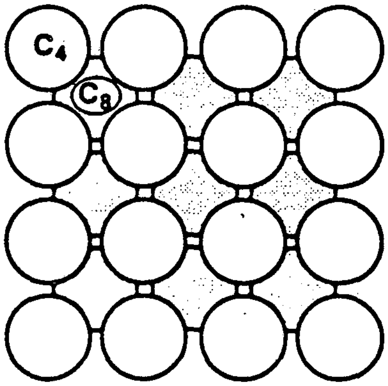

Fe(211)

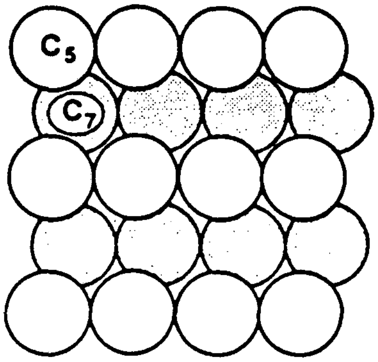

Fe(110)

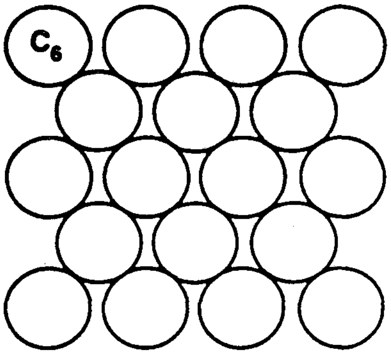

XBL 864-1664

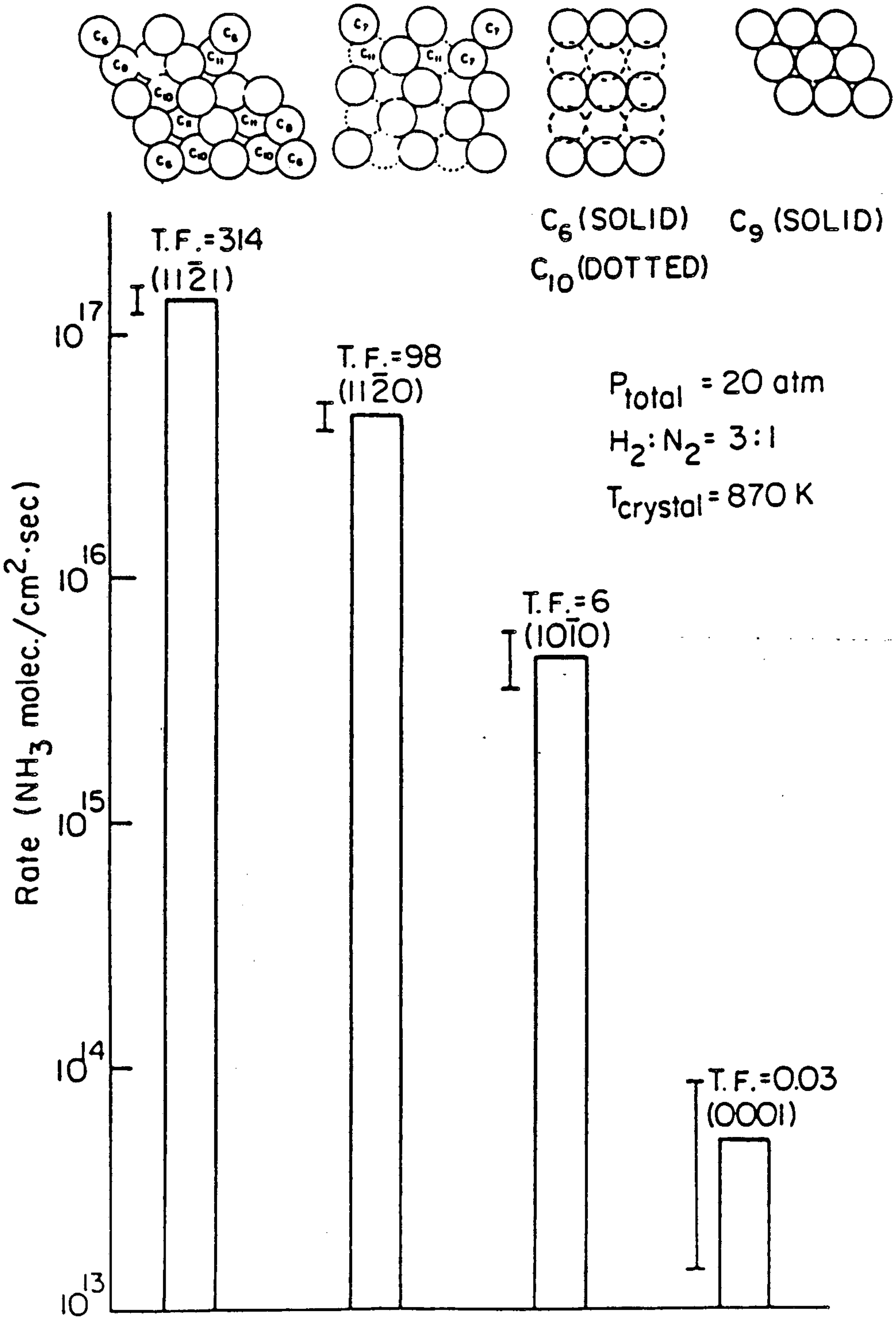
C6
C7
C8
C9
C10
C11
C6 (SOLID)
C10 (DOTTED)
C9 (SOLID)
T.F.=314
(11$\bar{2}$1)
T.F.=98
(11$\bar{2}$0)
T.F.=6
(10$\bar{1}$0)
T.F.=0.03
(0001)
P_{total} = 20 atm
$H_2:N_2$ = 3:1
$T_{crystal}$ = 870 K
Rate (NH_3 molec./$cm^2\cdot$sec)
10^{17}
10^{16}
10^{15}
10^{14}
10^{13}

XBL 845-1900

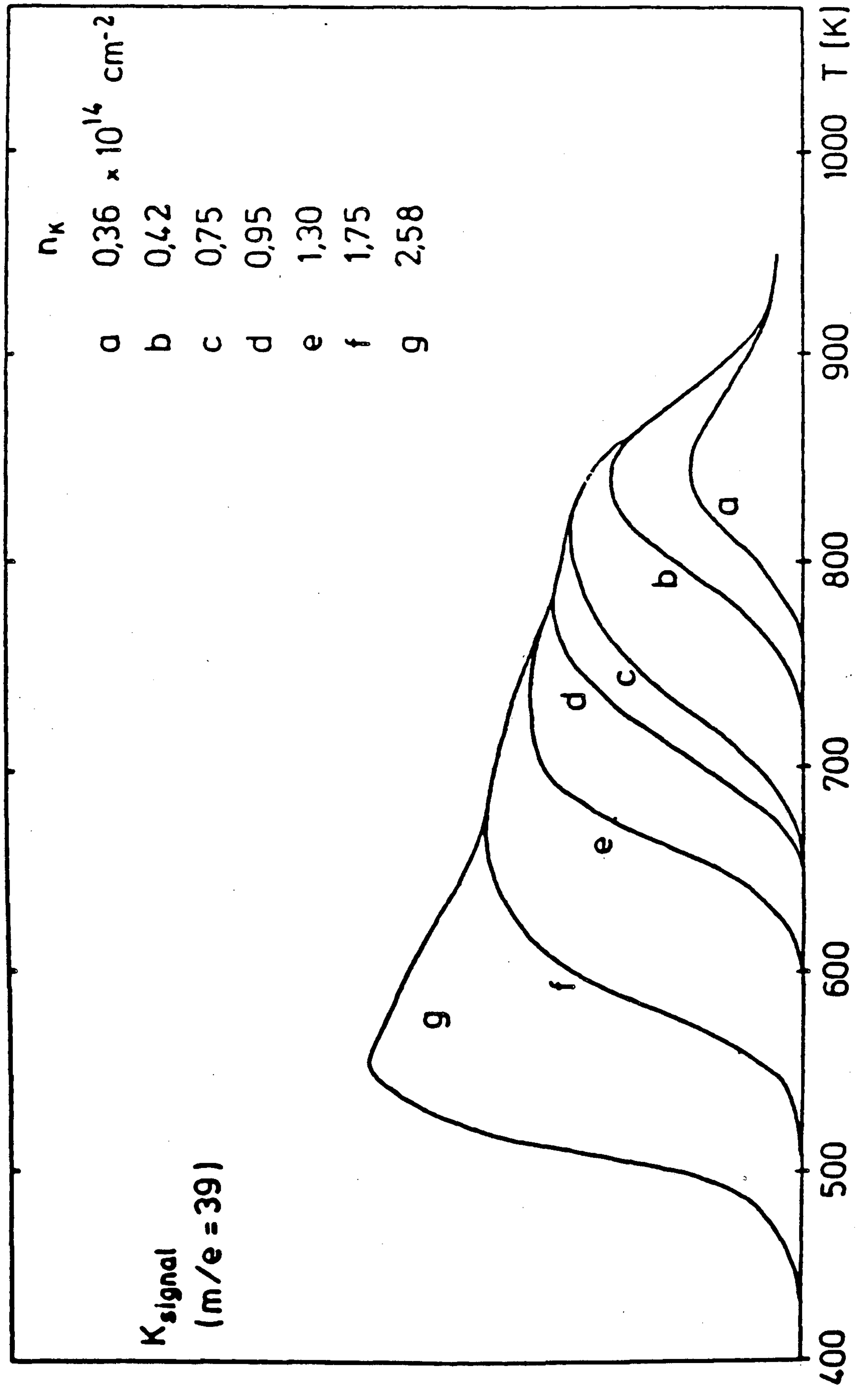

K_signal
(m/e = 39)
T [K]
400
500
600
700
800
900
1000
n_K
a 0,36 × 10^14 cm^-2
b 0,42
c 0,75
d 0,95
e 1,30
f 1,75
g 2,58
a
b
c
d
e
f
g

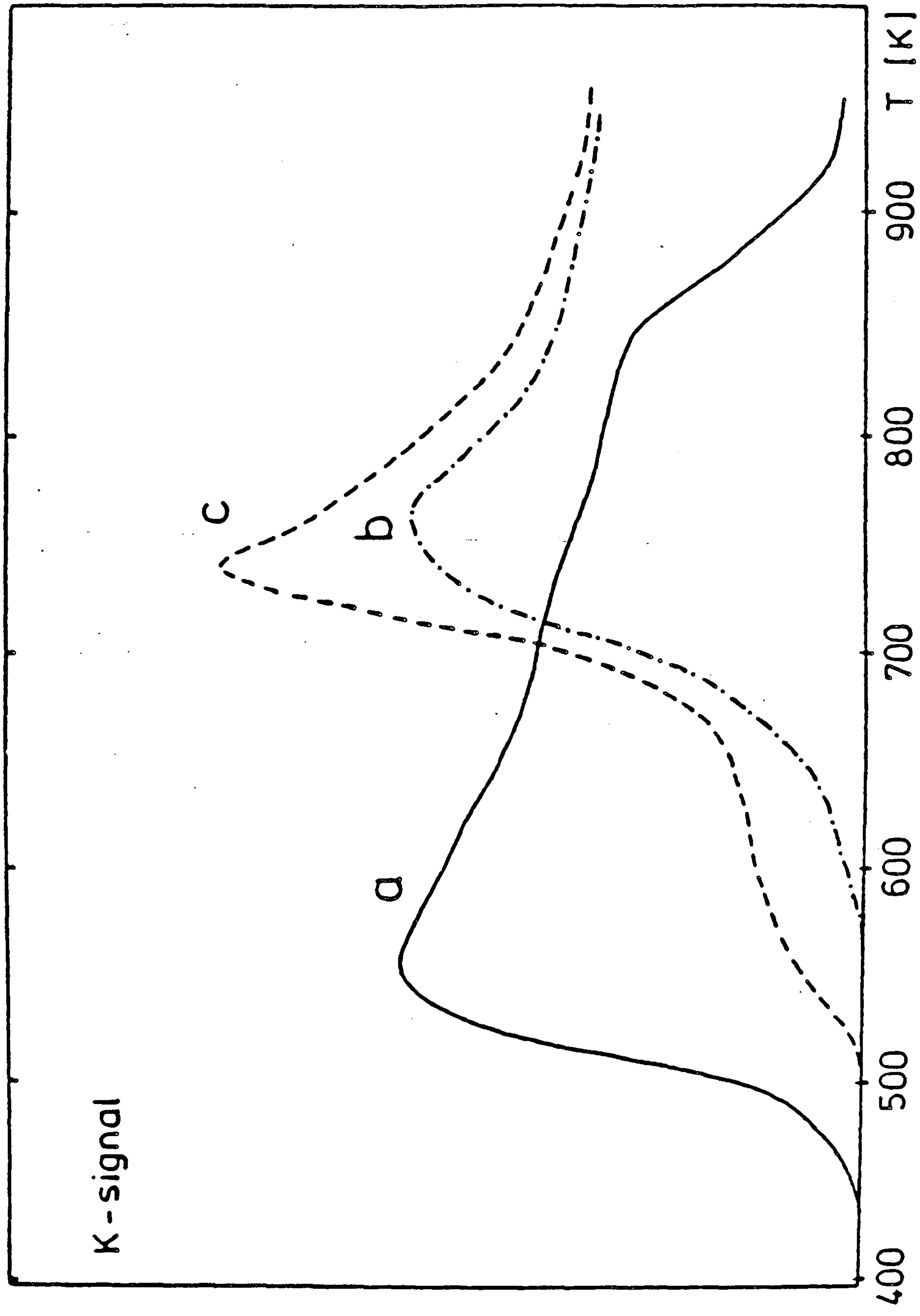
K - signal
T [K]
400
500
600
700
800
900
a
b
c

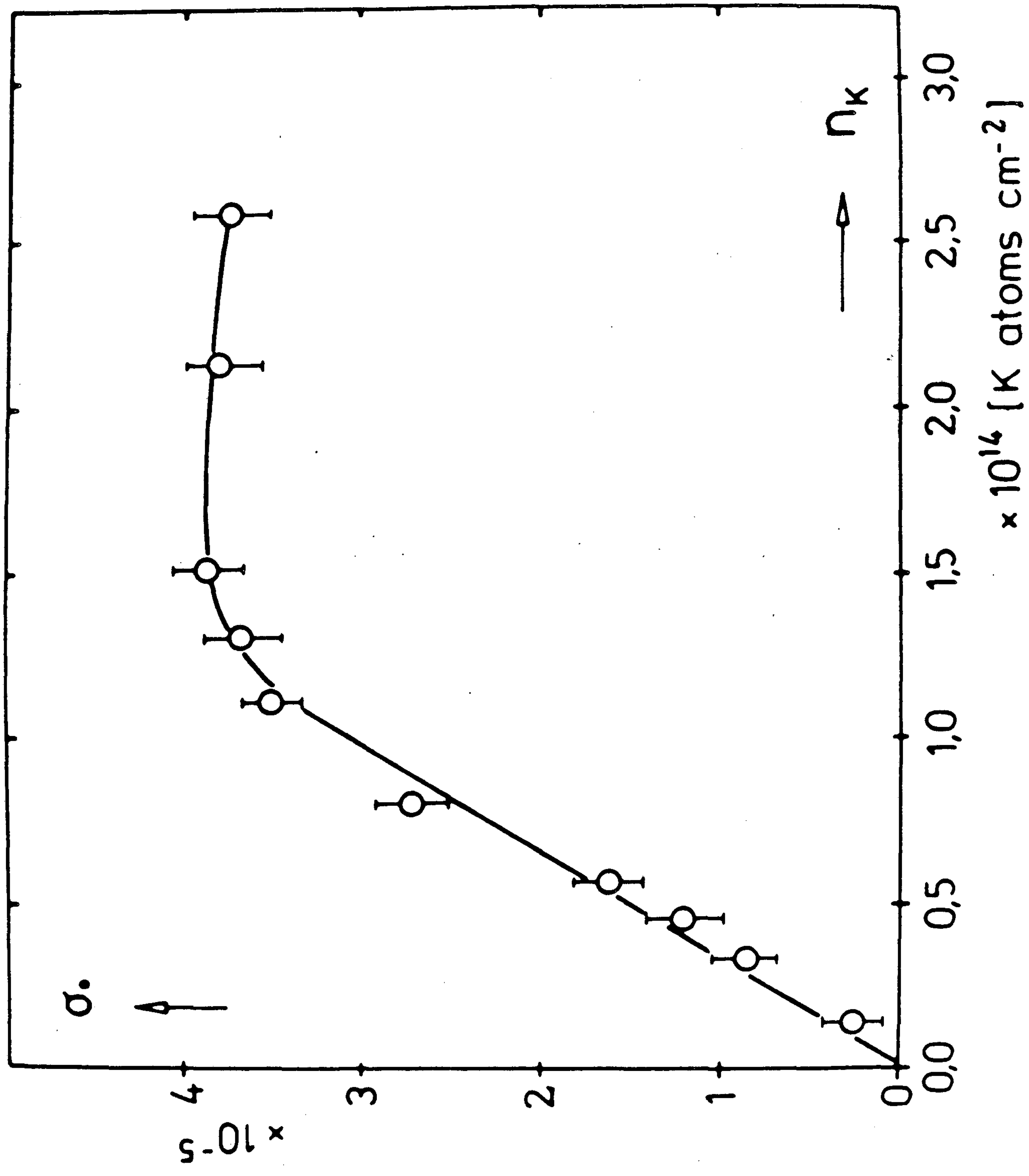

σ.
× 10⁻⁵
0
1
2
3
4
0,0
0,5
1,0
1,5
2,0
2,5
3,0
n_K
× 10¹⁴ [K atoms cm⁻²]

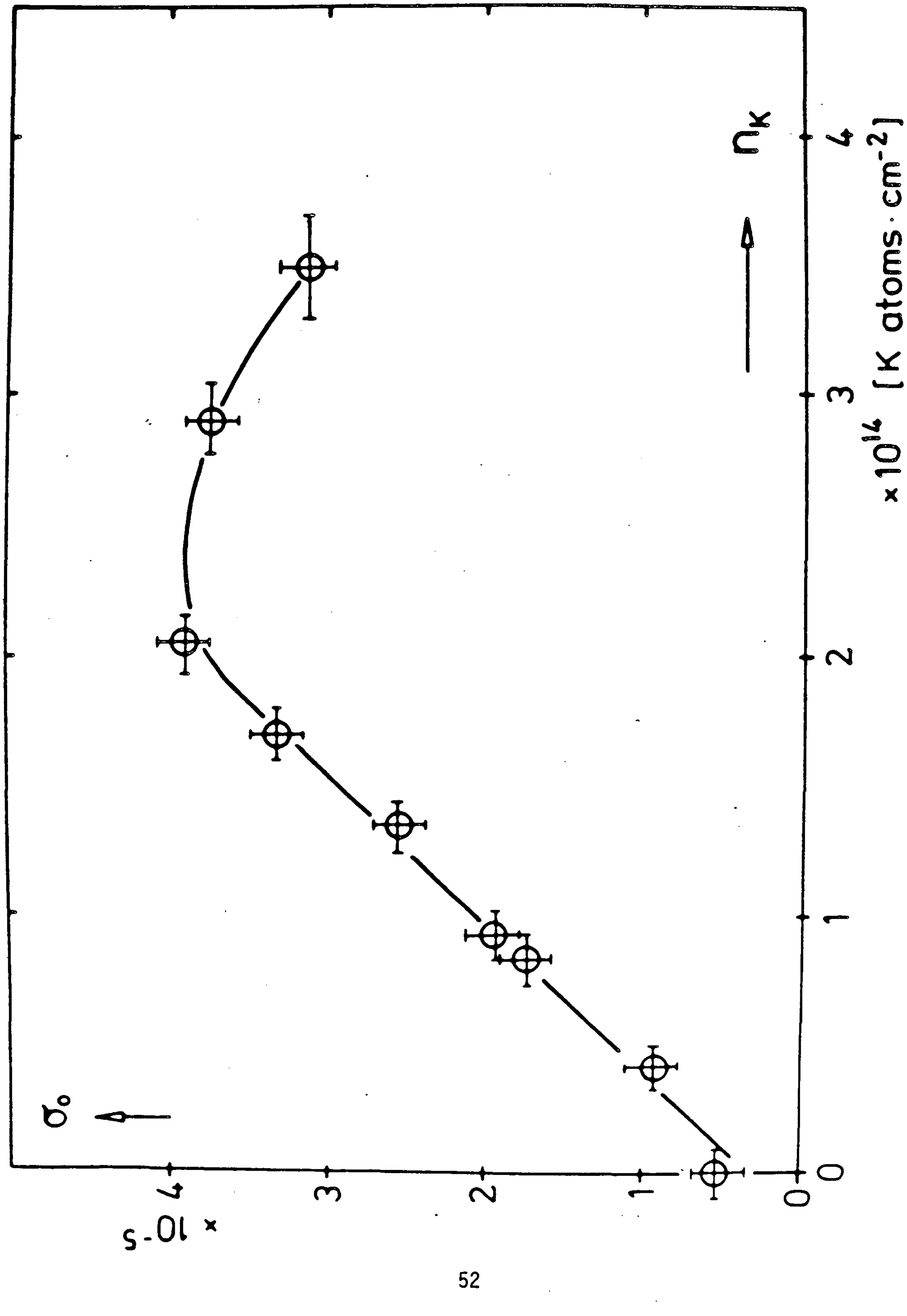
σ₀
× 10-5
0
1
2
3
4
0
1
2
3
4
× 10¹⁴ [K atoms · cm⁻²]
n_K

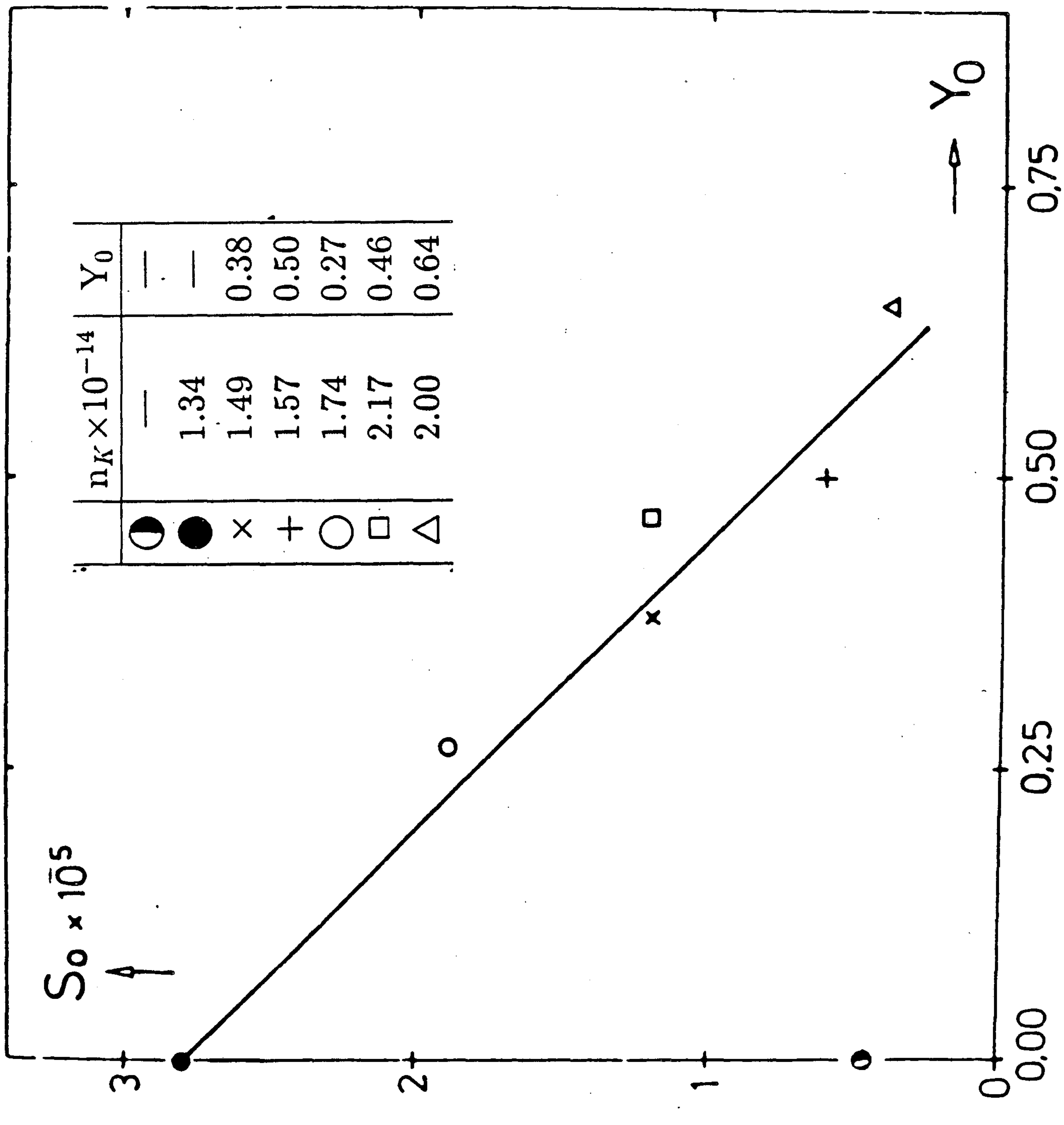

	$n_K \times 10^{-14}$	Y_0
◐	—	—
●	1.34	—
×	1.49	0.38
+	1.57	0.50
○	1.74	0.27
□	2.17	0.46
△	2.00	0.64

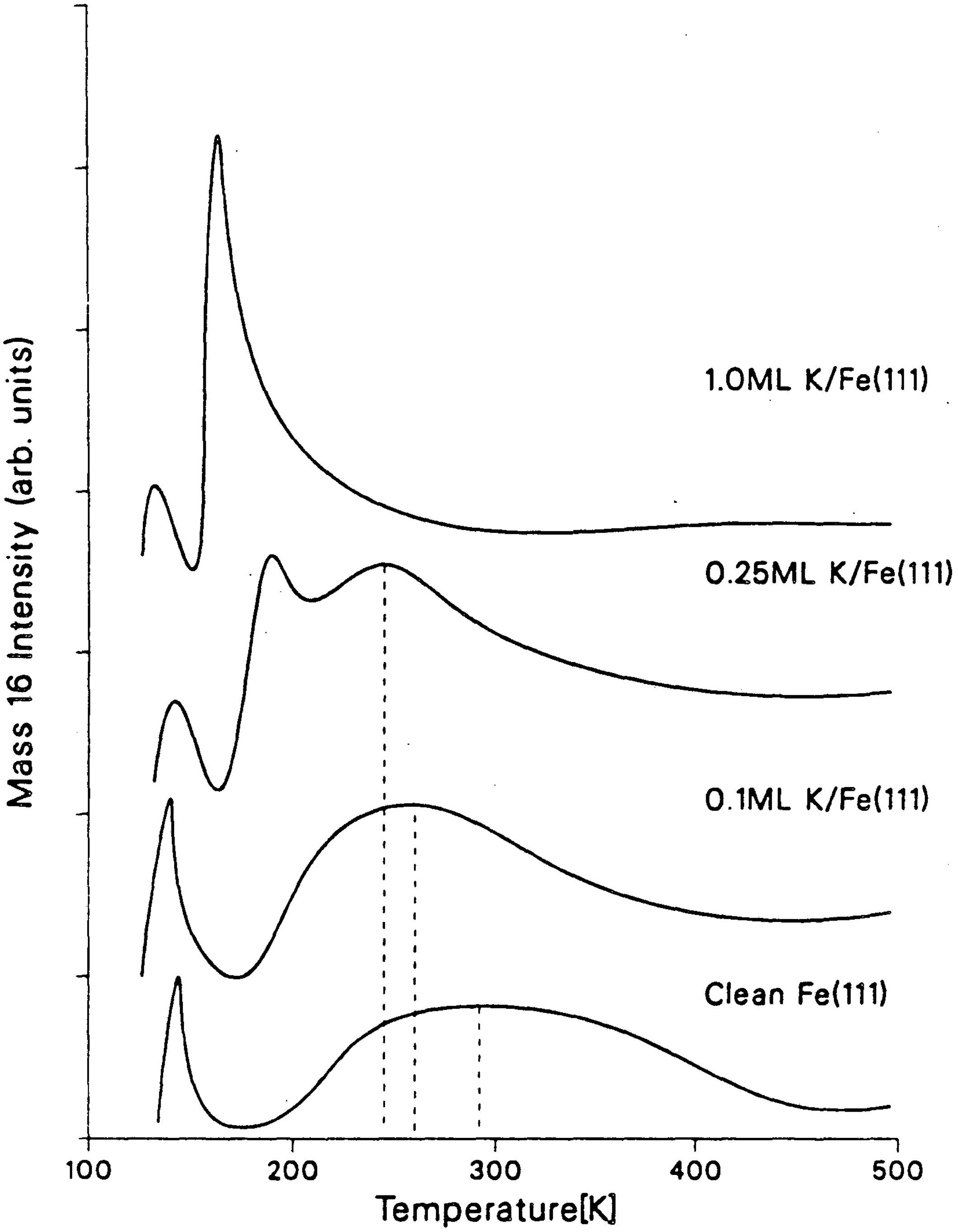
Mass 16 Intensity (arb. units)
1.0ML K/Fe(111)
0.25ML K/Fe(111)
0.1ML K/Fe(111)
Clean Fe(111)
100
200
300
400
500
Temperature[K]

XBL 873-1254

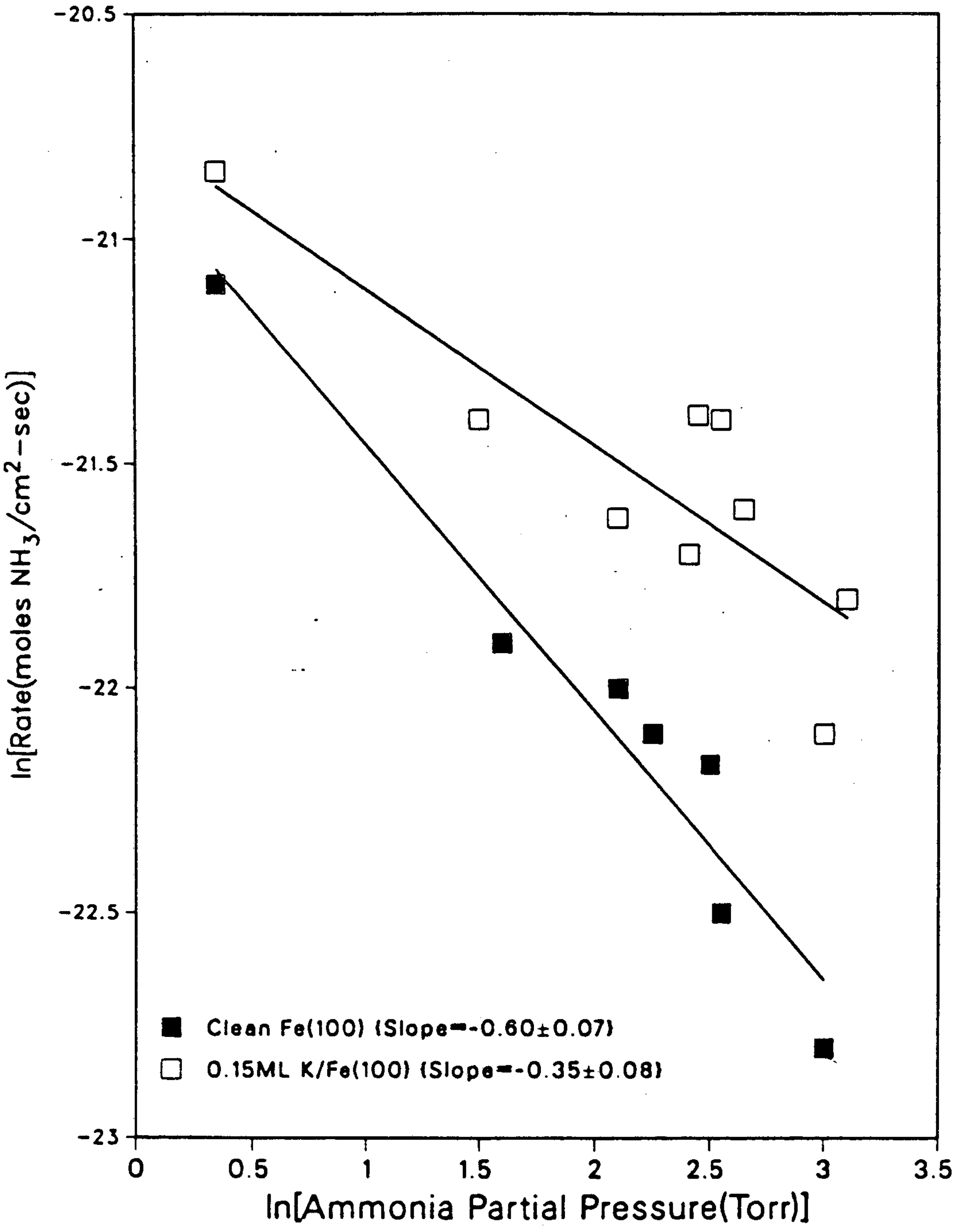
-20.5
-21
-21.5
-22
-22.5
-23
0
0.5
1
1.5
2
2.5
3
3.5
ln[Rate(moles NH₃/cm²-sec)]
ln[Ammonia Partial Pressure(Torr)]
■ Clean Fe(100) (Slope=-0.60±0.07)
□ 0.15ML K/Fe(100) (Slope=-0.35±0.08)

XBL 873-1251

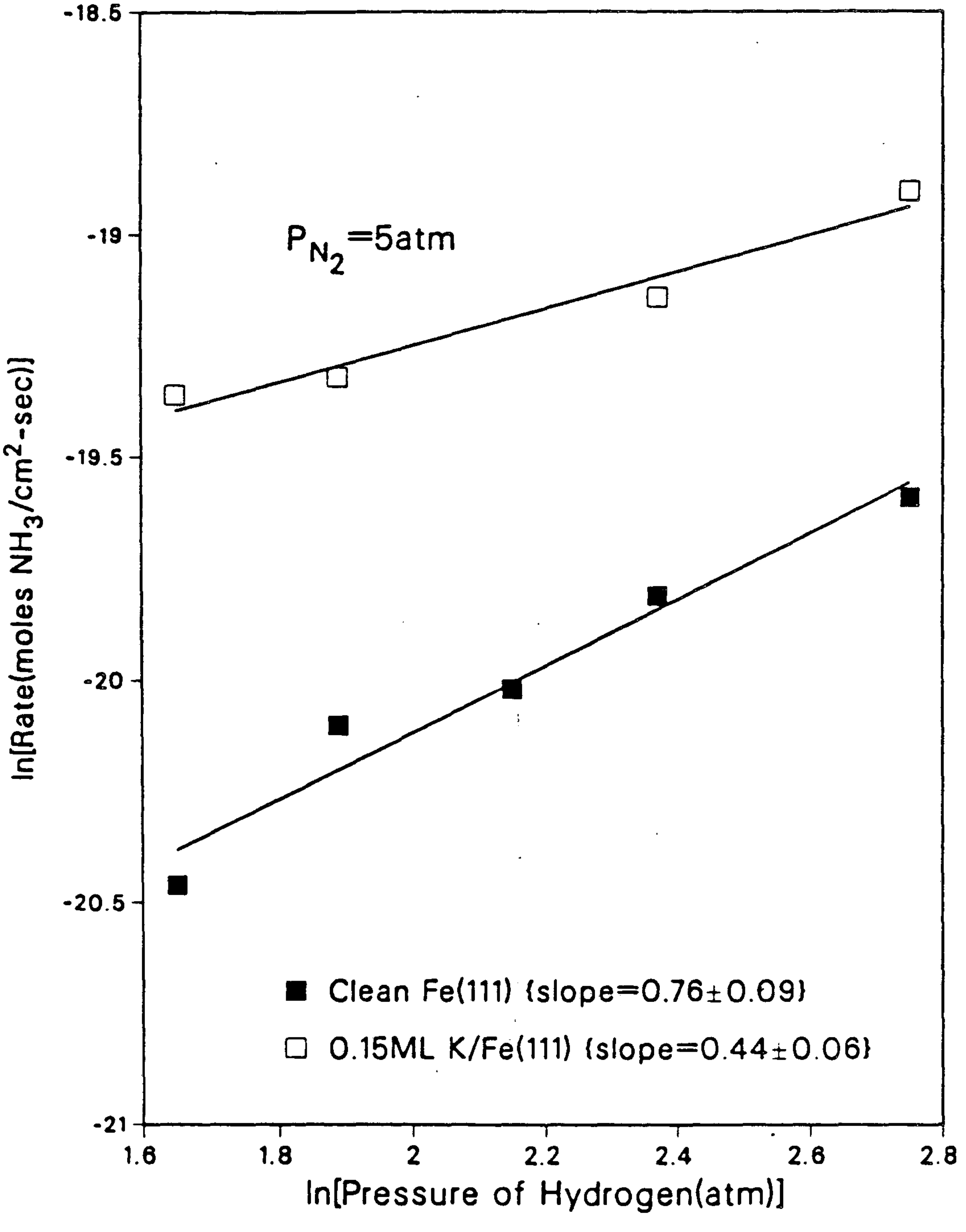

-18.5
-19
-19.5
-20
-20.5
-21
1.6
1.8
2
2.2
2.4
2.6
2.8
P_{N_2}=5atm
ln[Rate(moles NH_3/cm^2-sec)]
ln[Pressure of Hydrogen(atm)]
■ Clean Fe(111) (slope=0.76±0.09)
□ 0.15ML K/Fe(111) (slope=0.44±0.06)

XBL 873-1252

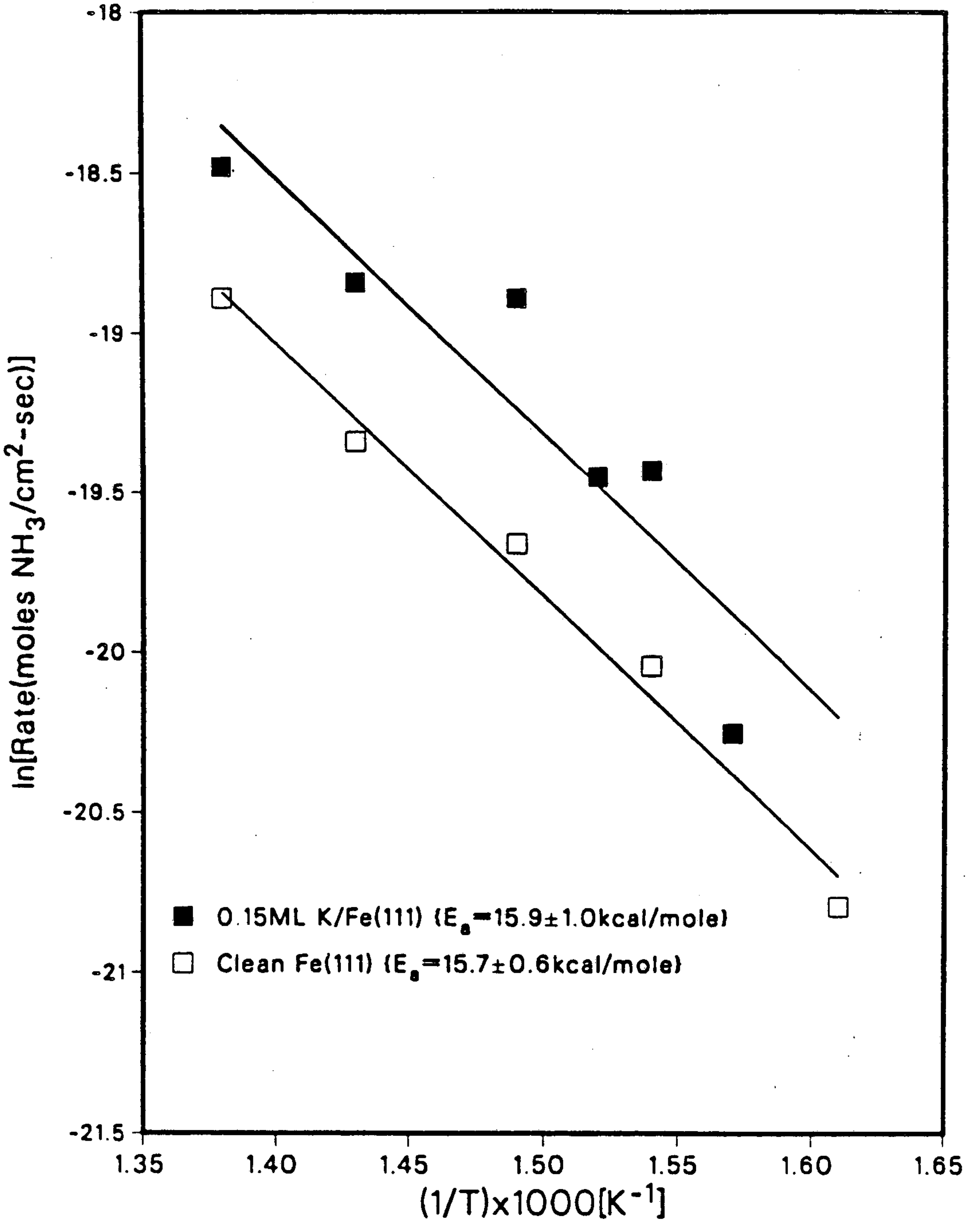
-18
-18.5
-19
-19.5
-20
-20.5
-21
-21.5
1.35
1.40
1.45
1.50
1.55
1.60
1.65
$\ln[\mathrm{Rate(moles\ NH_3/cm^2\text{-}sec)}]$
$(1/T)\times 1000[K^{-1}]$
■ 0.15ML K/Fe(111) (E_a=15.9±1.0kcal/mole)
□ Clean Fe(111) (E_a=15.7±0.6kcal/mole)

XBL 873-1253

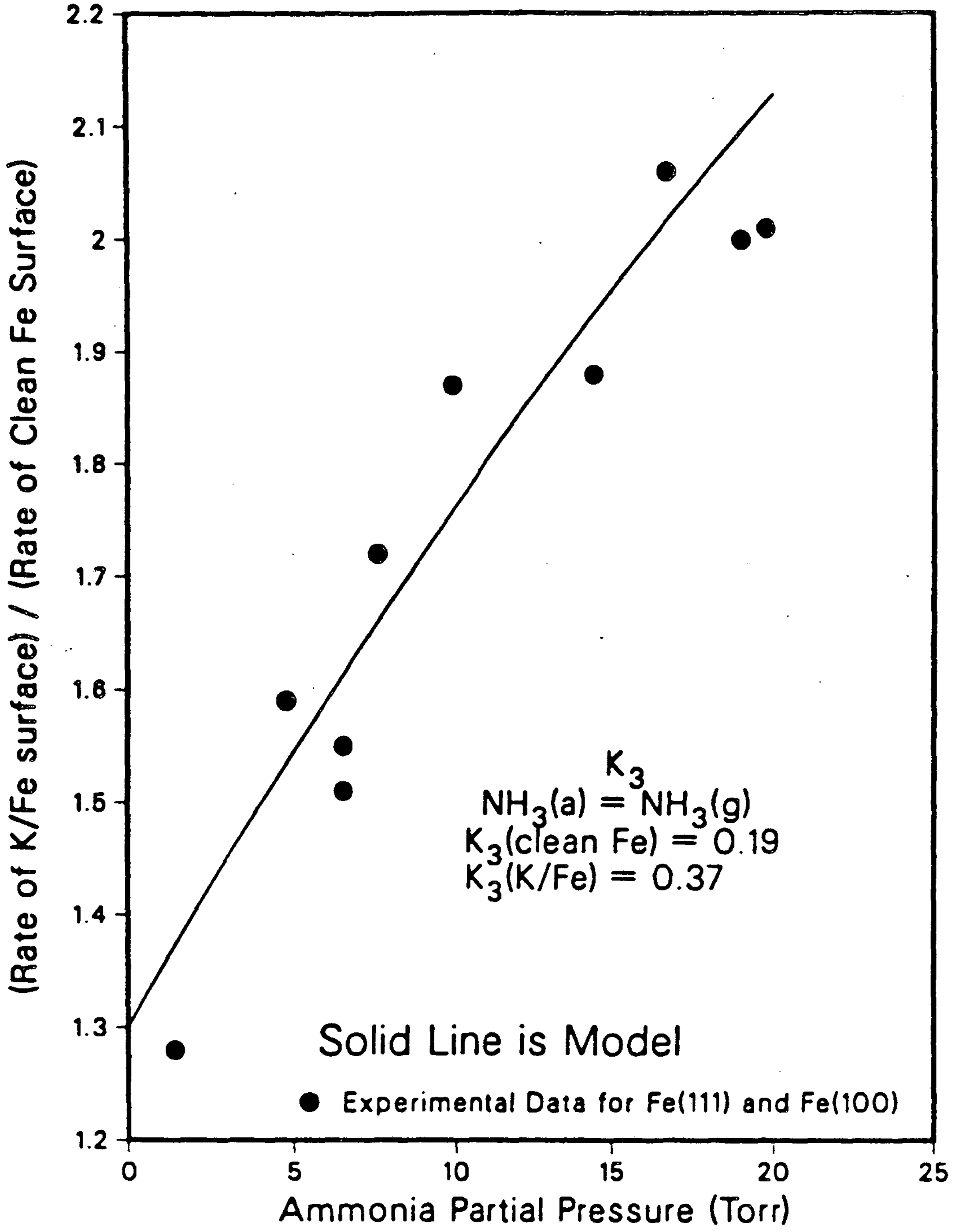
2.2
2.1
2
1.9
1.8
1.7
1.6
1.5
1.4
1.3
1.2
(Rate of K/Fe surface) / (Rate of Clean Fe Surface)
0
5
10
15
20
25
Ammonia Partial Pressure (Torr)
$NH_3(a) \overset{K_3}{=} NH_3(g)$
K_3(clean Fe) = 0.19
K_3(K/Fe) = 0.37
Solid Line is Model
● Experimental Data for Fe(111) and Fe(100)

XBL 873-1255

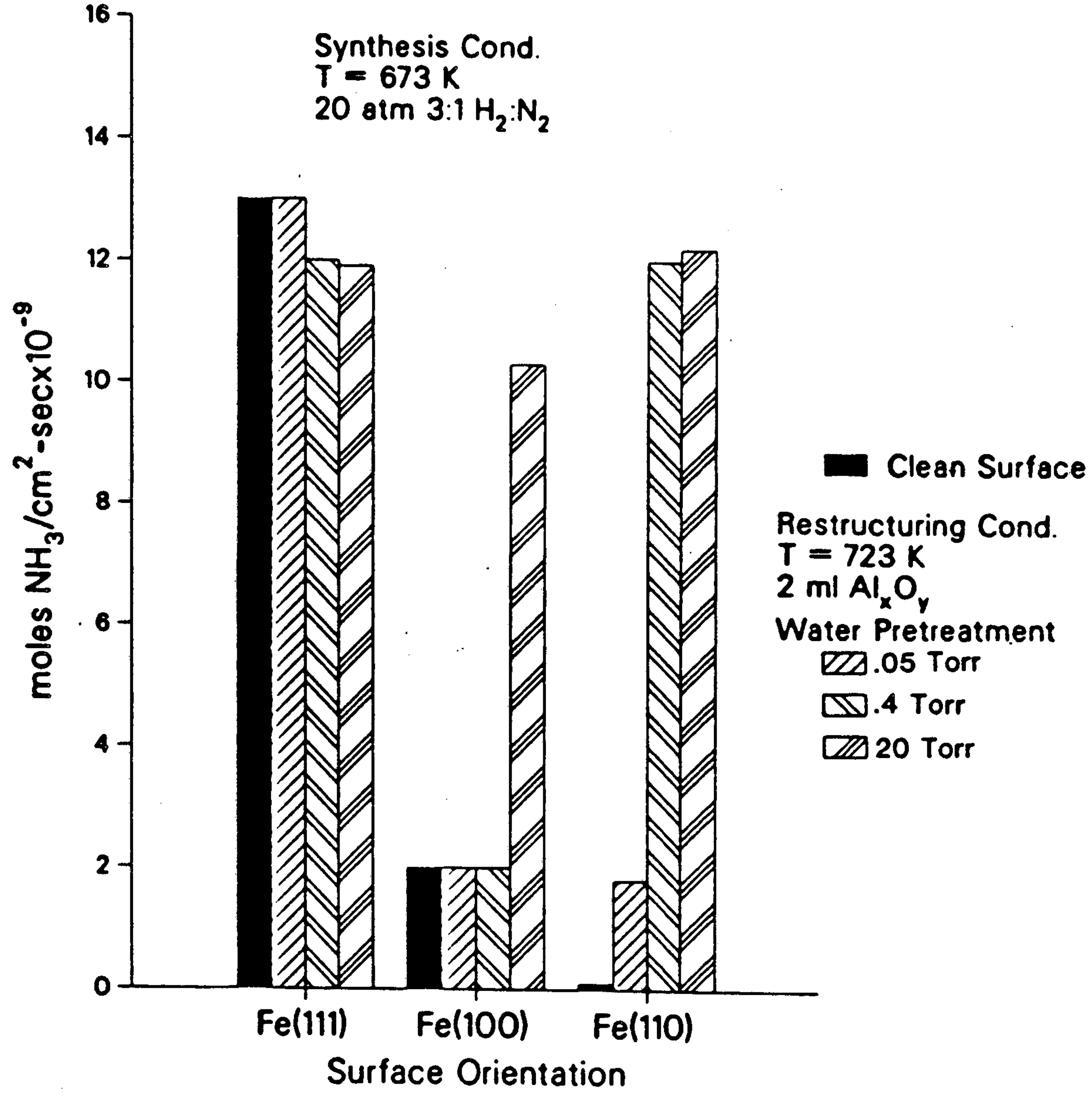
16
14
12
10
8
6
4
2
0
moles NH$_3$/cm^2-secx10^{-9}
Synthesis Cond.
T = 673 K
20 atm 3:1 H$_2$:N$_2$
Fe(111)
Fe(100)
Fe(110)
Surface Orientation
Clean Surface
Restructuring Cond.
T = 723 K
2 ml Al$_x$O$_y$
Water Pretreatment
.05 Torr
.4 Torr
20 Torr

XBL 868-3128

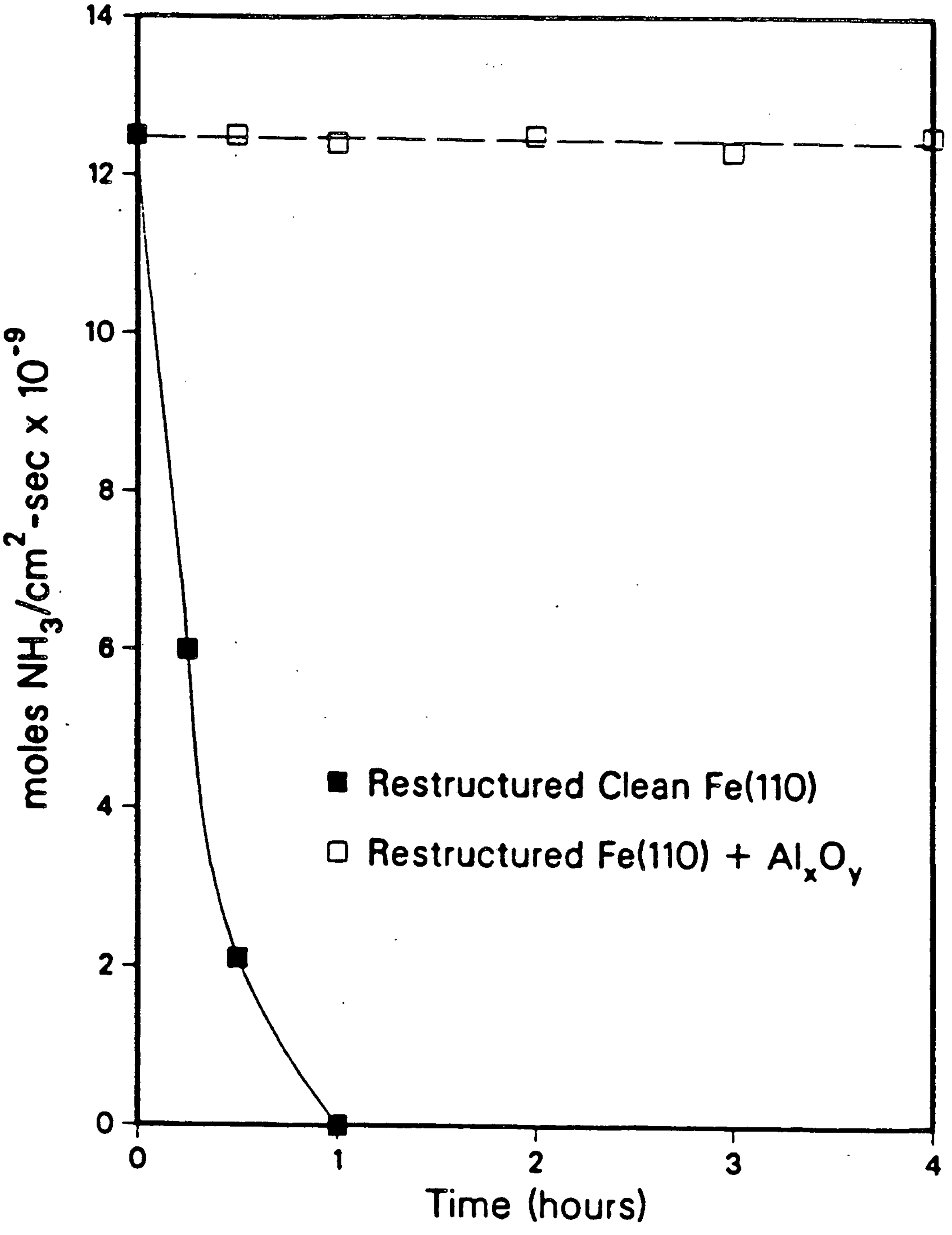
14
12
10
8
6
4
2
0
moles NH_3/cm^2-sec x 10^{-9}
0
1
2
3
4
Time (hours)
■ Restructured Clean Fe(110)
□ Restructured Fe(110) + Al_xO_y

XBL 865-1956

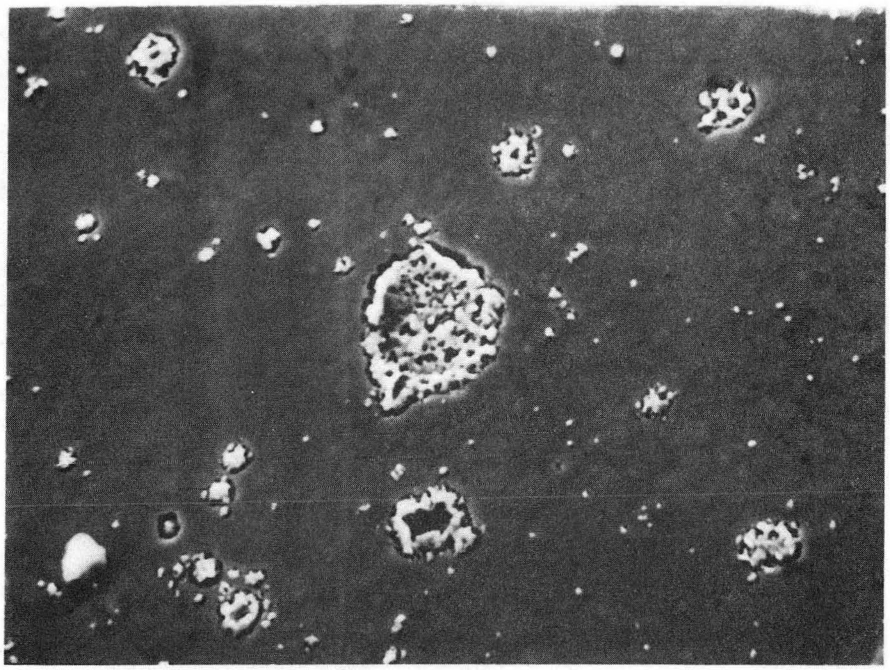

a

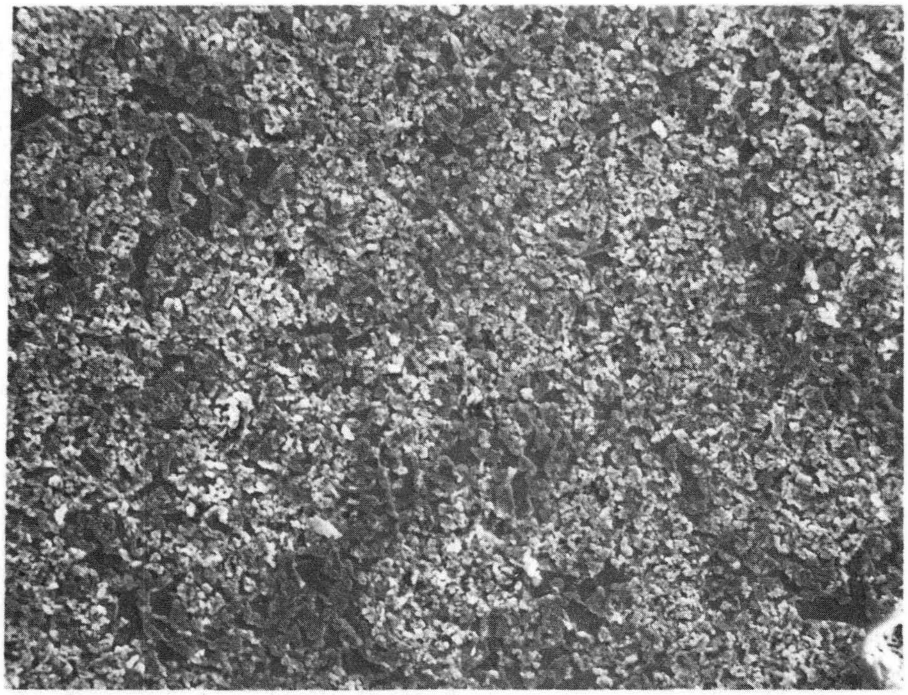

b

XBB 866-4791

10μm

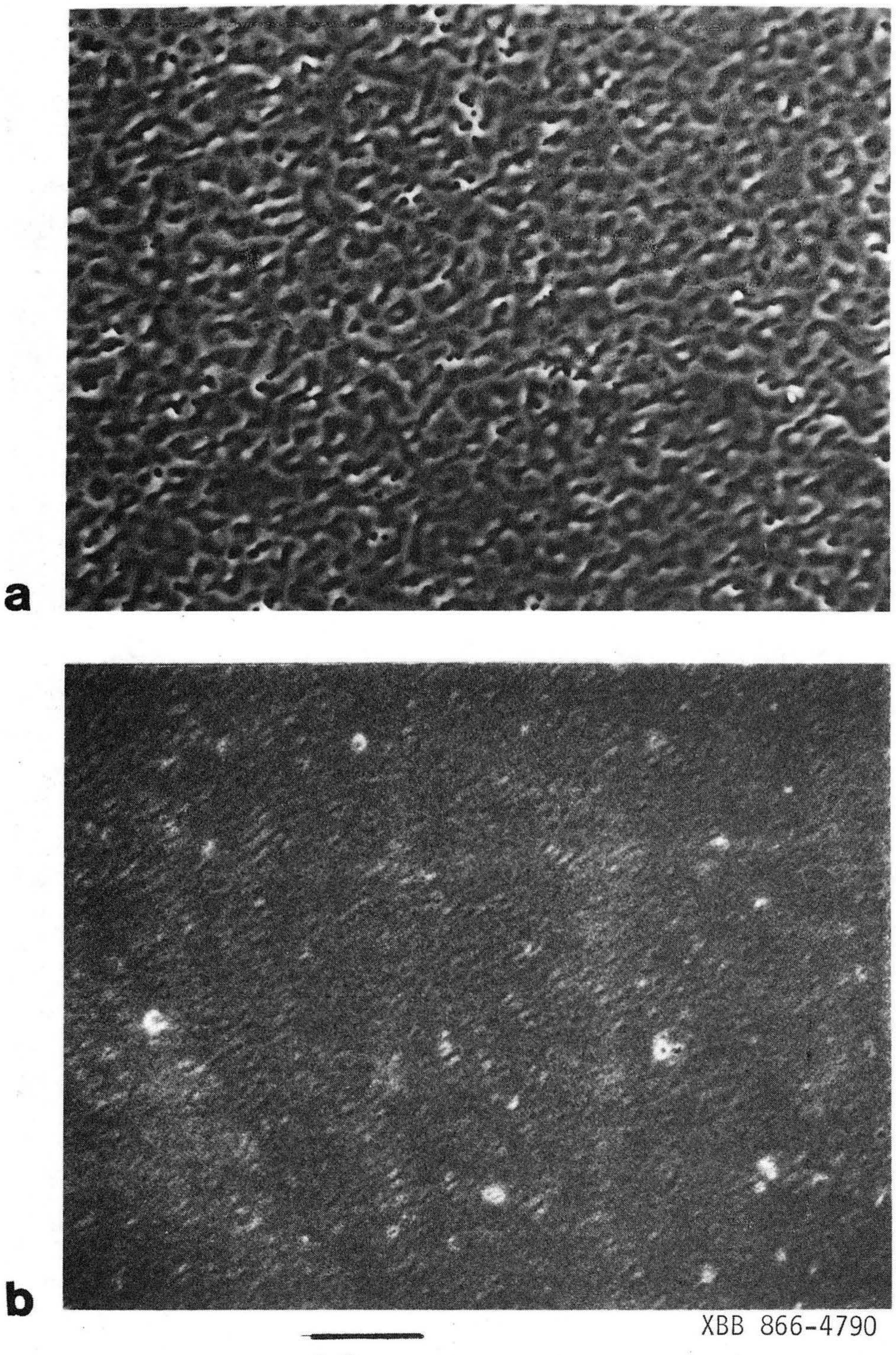

XBB 866-4790

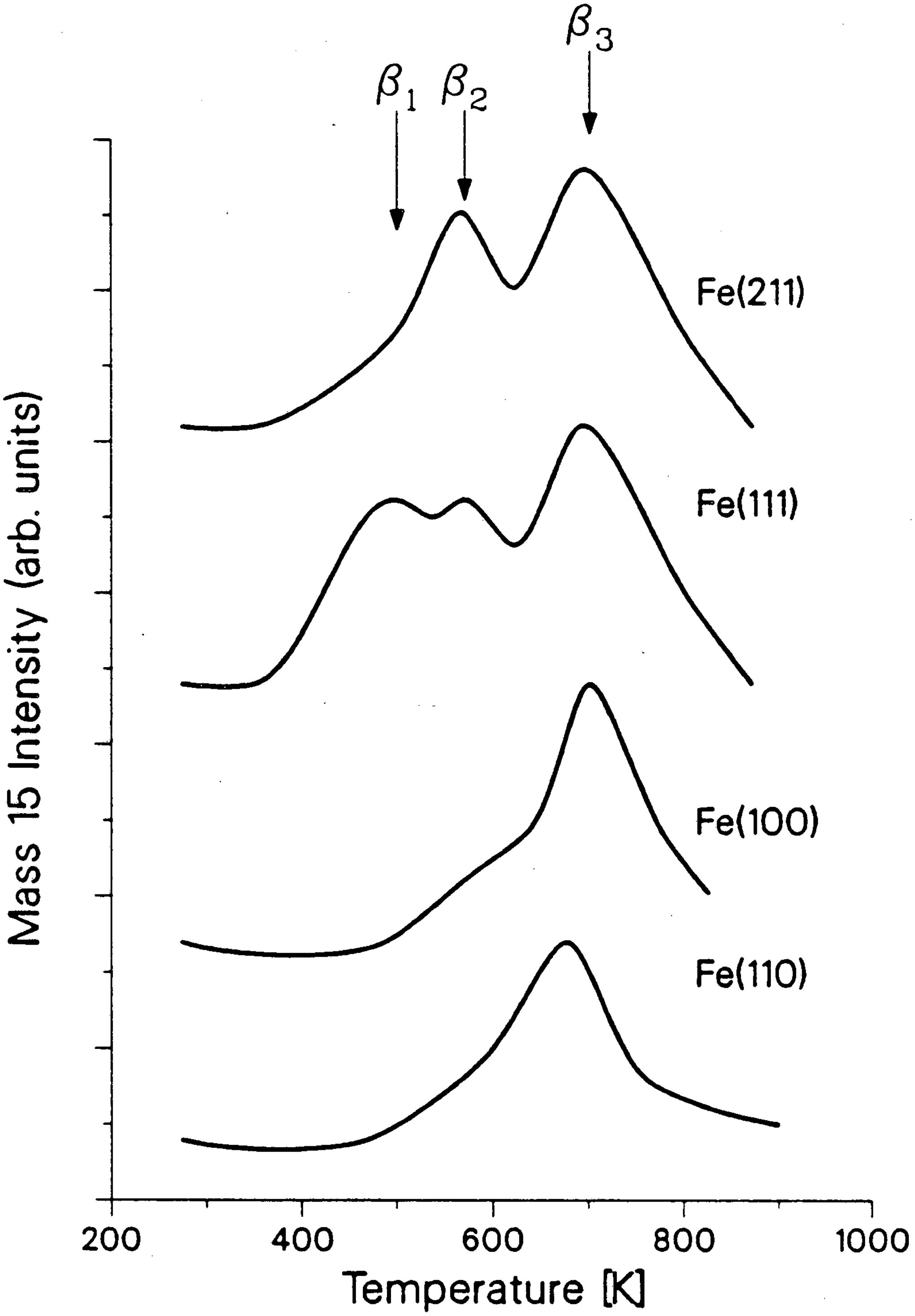
β_1
β_2
β_3
Fe(211)
Fe(111)
Fe(100)
Fe(110)
Mass 15 Intensity (arb. units)
200
400
600
800
1000
Temperature [K]

XBL 866-2297

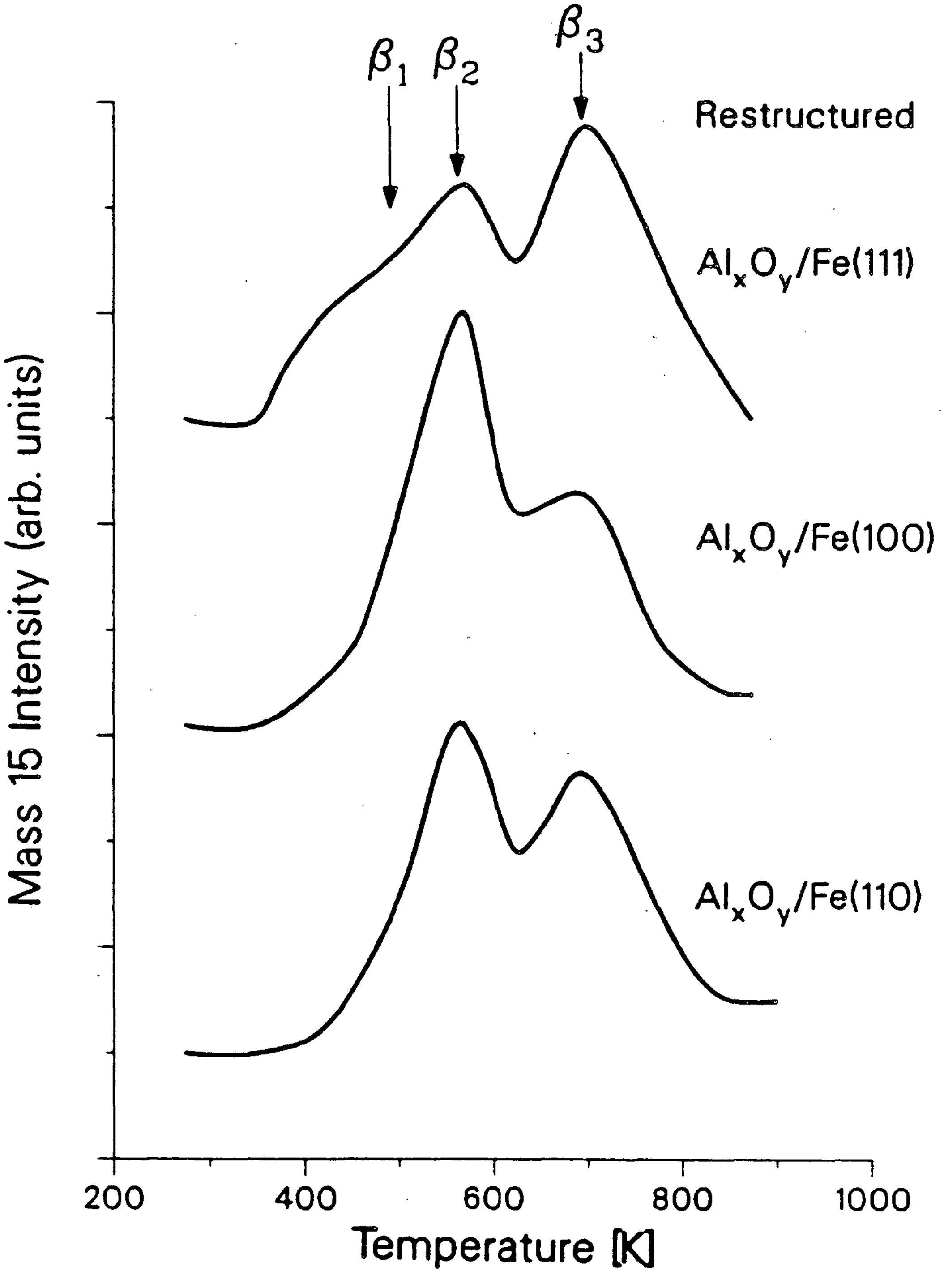
β_1
β_2
β_3
Restructured
Al_xO_y/Fe(111)
Al_xO_y/Fe(100)
Al_xO_y/Fe(110)
Mass 15 Intensity (arb. units)
200
400
600
800
1000
Temperature [K]

XBL 866-2296

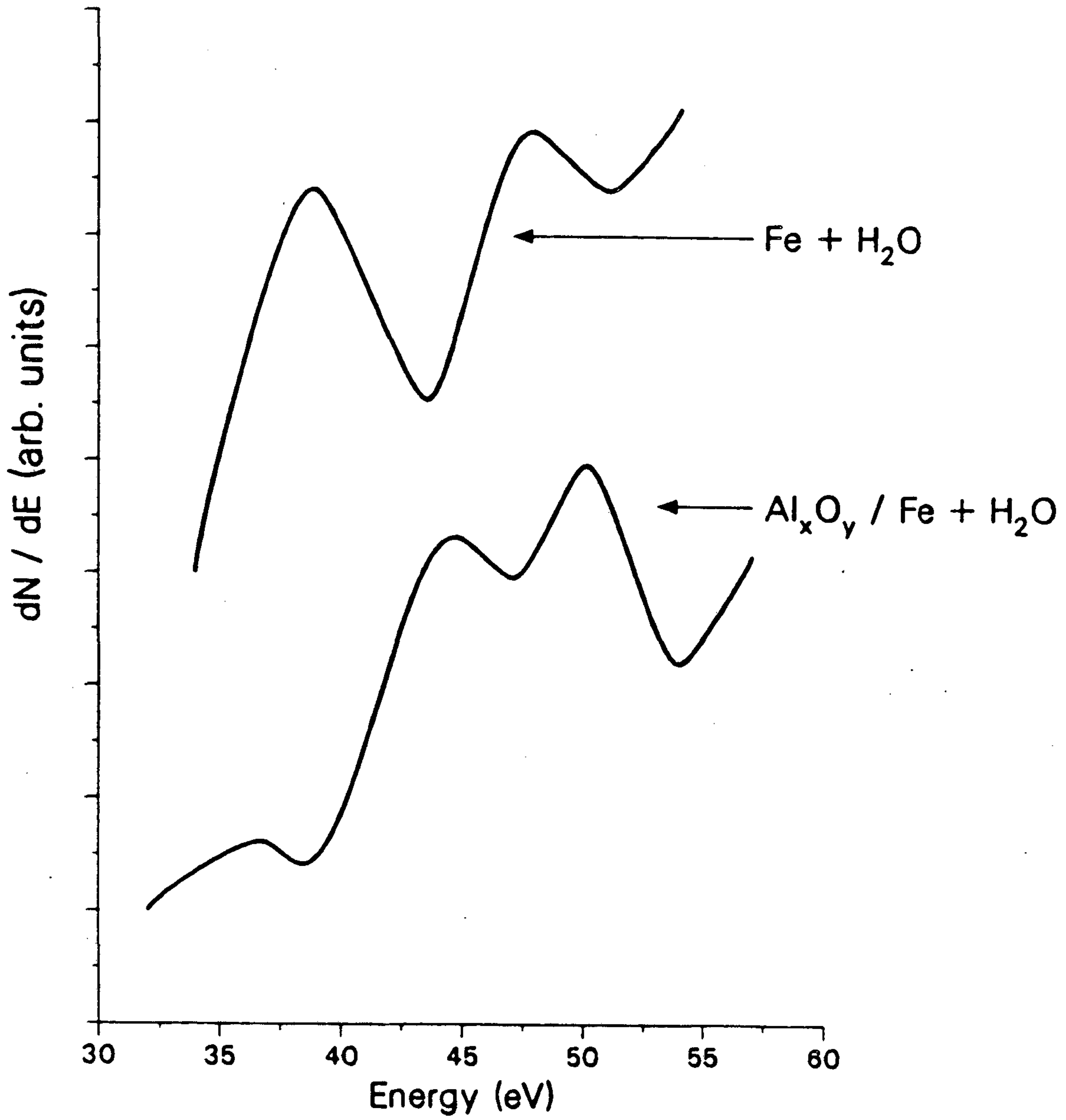

XBL 866-2294

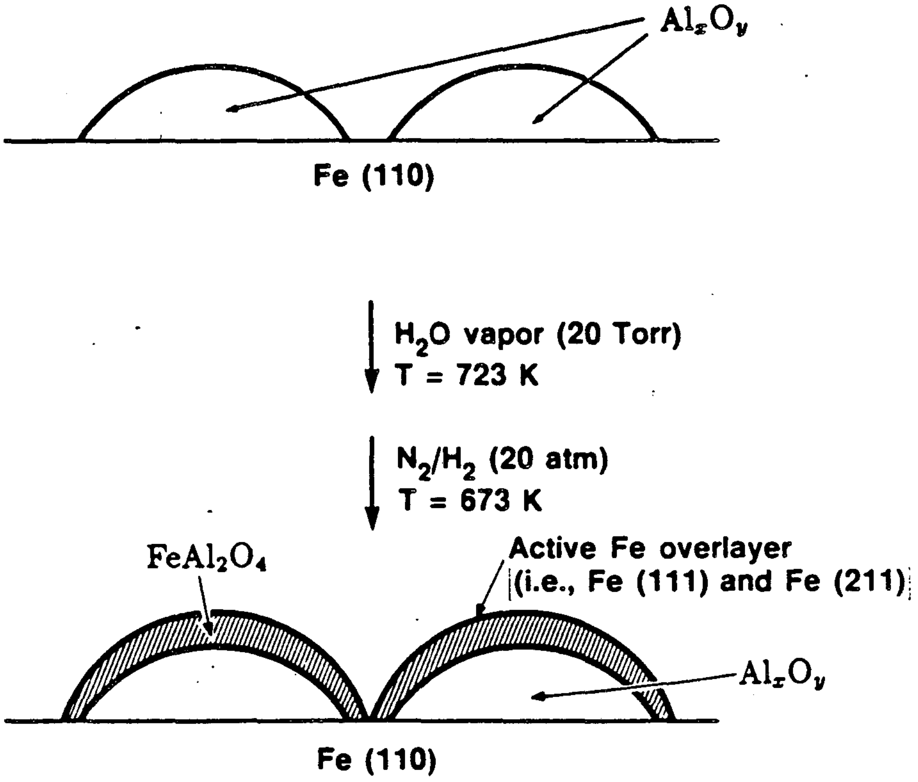
Al_xO_y
Fe (110)
H_2O vapor (20 Torr)
T = 723 K
N_2/H_2 (20 atm)
T = 673 K
$FeAl_2O_4$
Active Fe overlayer
(i.e., Fe (111) and Fe (211))
Al_xO_y
Fe (110)

XBL 871-337

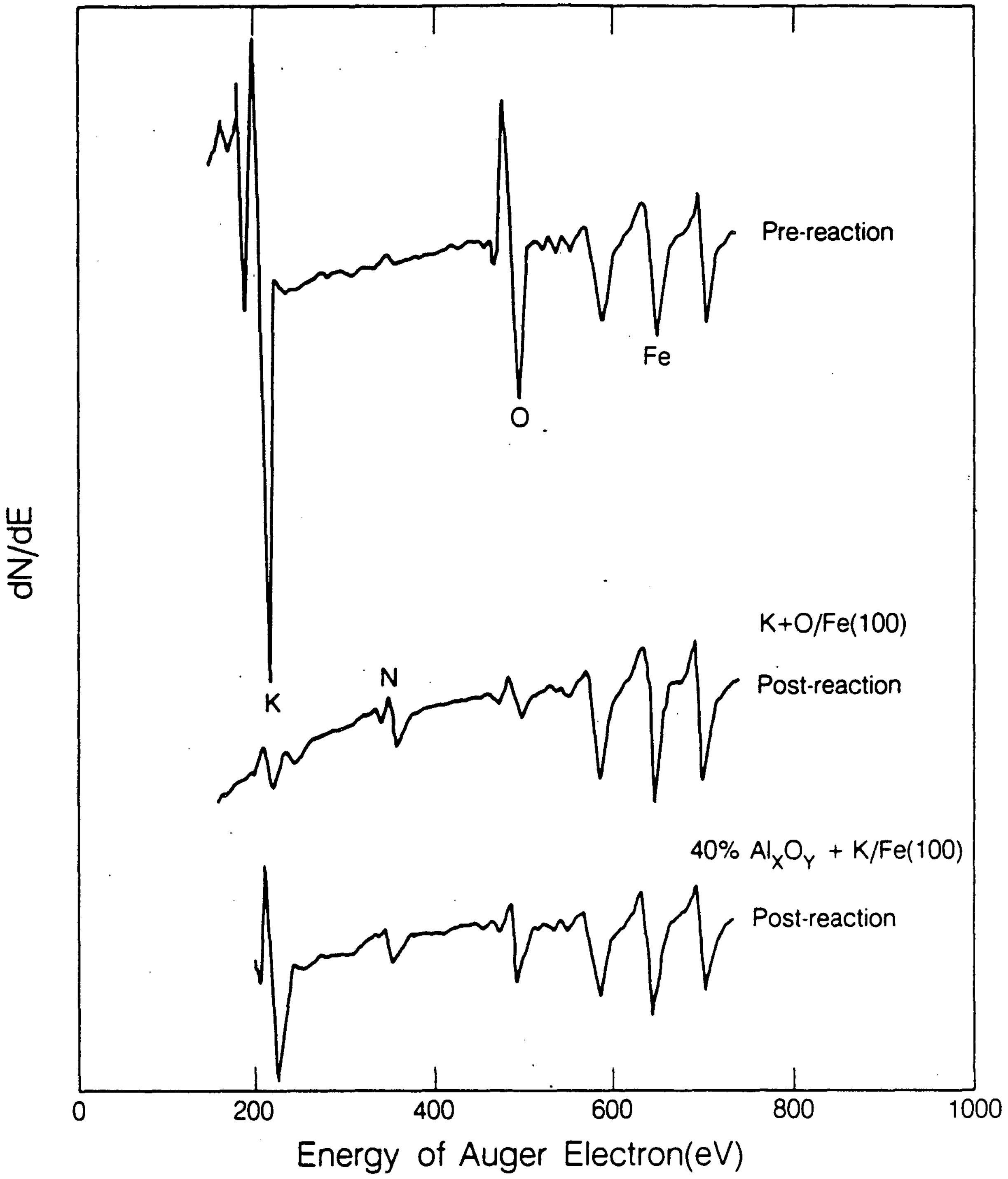
dN/dE
Pre-reaction
Fe
O
K+O/Fe(100)
Post-reaction
N
K
40% Al_XO_Y + K/Fe(100)
Post-reaction
0
200
400
600
800
1000
Energy of Auger Electron(eV)

XBL 858-8961

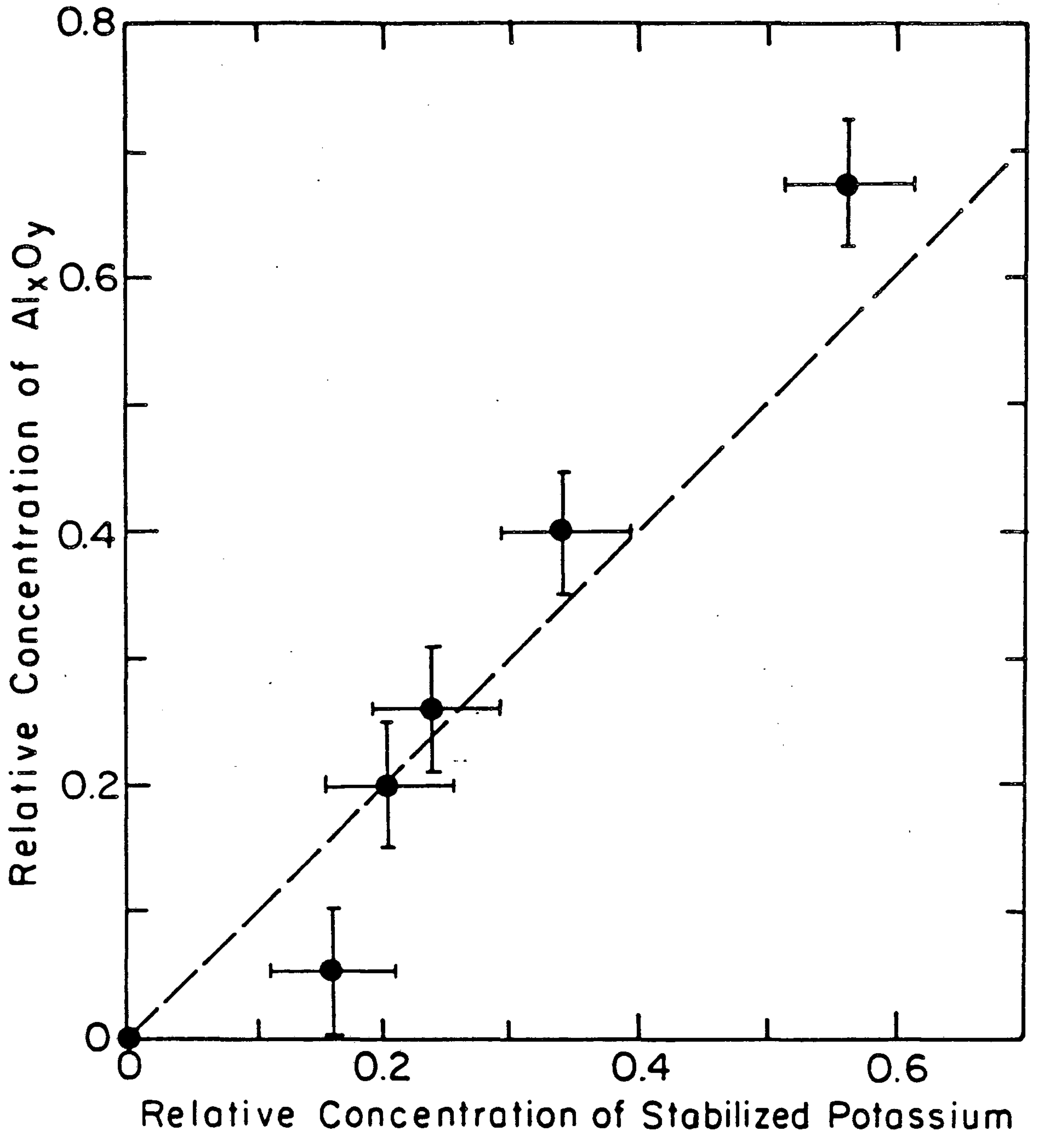

XBL 8512-6873A

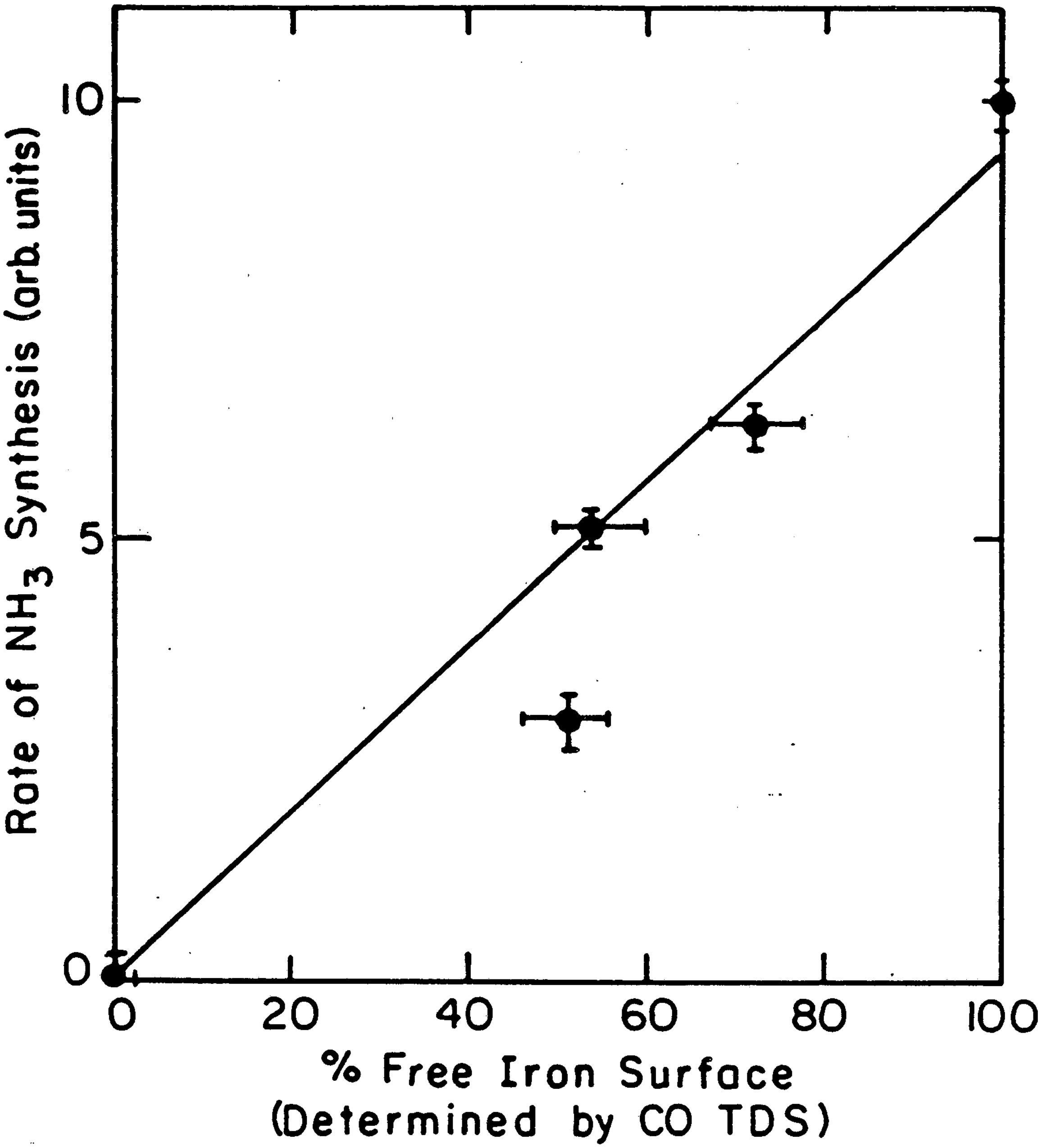
Rate of NH₃ Synthesis (arb. units)
10
5
0
0
20
40
60
80
100
% Free Iron Surface
(Determined by CO TDS)

XBL858-6578

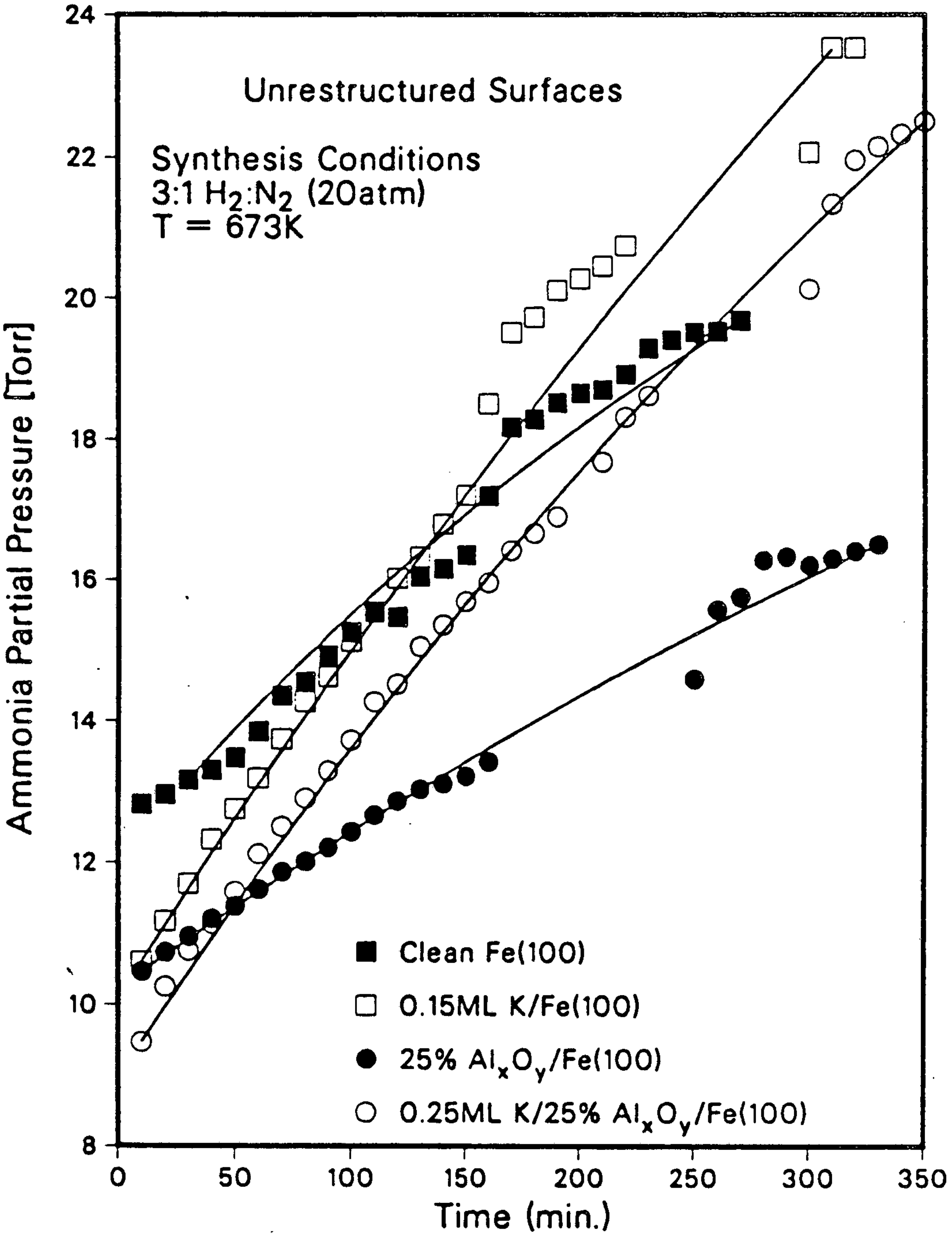
Unrestructured Surfaces
Synthesis Conditions
3:1 H_2:N_2 (20atm)
T = 673K
Ammonia Partial Pressure [Torr]
Time (min.)
24
22
20
18
16
14
12
10
8
0
50
100
150
200
250
300
350
■ Clean Fe(100)
☐ 0.15ML K/Fe(100)
● 25% Al_xO_y/Fe(100)
○ 0.25ML K/25% Al_xO_y/Fe(100)

XBL 874-1507

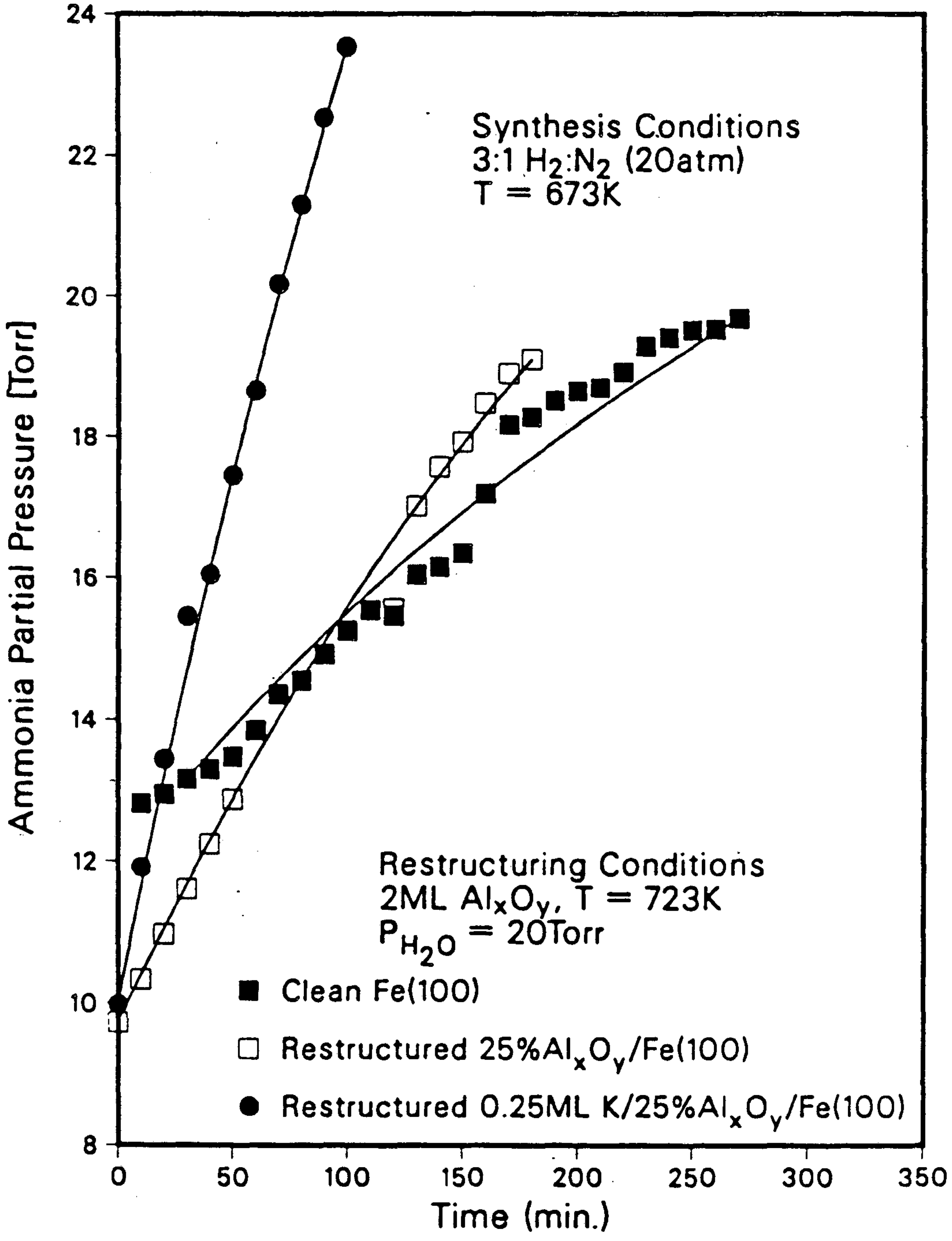
24
22
20
18
16
14
12
10
8
Ammonia Partial Pressure [Torr]
0
50
100
150
200
250
300
350
Time (min.)
Synthesis Conditions
3:1 H_2:N_2 (20atm)
T = 673K
Restructuring Conditions
2ML Al_xO_y, T = 723K
P_{H_2O} = 20Torr
■ Clean Fe(100)
□ Restructured 25%Al_xO_y/Fe(100)
● Restructured 0.25ML K/25%Al_xO_y/Fe(100)

XBL 874-1506

LAWRENCE BERKELEY LABORATORY
TECHNICAL INFORMATION DEPARTMENT
UNIVERSITY OF CALIFORNIA
BERKELEY, CALIFORNIA 94720